Anti-tumor effects of an aqueous extract of *Ecklonia cava* in BALB/cKorl syngeneic mice using colon carcinoma CT26 cells

JEONG EUN GONG[1], JI EUN KIM[1], SO HAE PARK[1], SU JIN LEE[1], YUN JU CHOI[1], SUN IL CHOI[2], YOUNG WHAN CHOI[3], HEE SEOB LEE[4], JIN TAE HONG[5] and DAE YOUN HWANG[1]

[1]Department of Biomaterials Science (BK21 FOUR Program), College of Natural Resources & Life Science/Life and Industry Convergence Research Institute/Laboratory Animal Resources Center, Pusan National University, Miryang 50463, Republic of Korea; [2]School of Pharmacy, Henan University, Henan 475004, P.R. China; [3]Department of Horticultural Bioscience, College of Natural Resources and Life Science, Pusan National University, Miryang 50463; [4]Department of Food Science and Nutrition, College of Human Ecology, Pusan National University, Busan 46241; [5]College of Pharmacy, Chungbuk National University, Chungju 28644, Republic of Korea

Received November 8, 2022; Accepted March 23, 2023

DOI: 10.3892/or.2023.8565

Abstract. *Ecklonia cava* (*E. cava*) is well known as one of edible alga that contains various unique polyphenols. The anti-tumor activity of an aqueous extract of *E. cava* (AEC) against colon carcinoma was evaluated by analyzing the alterations in tumor growth, histopathological structure and molecular mechanisms in CT26 tumor-bearing BALB/cKorl syngeneic mice after administrating AEC for five weeks. AEC contained high total phenolic contents and demonstrated significant scavenging activity against 2,2-diphenyl-1-picrylhydrazyl radicals. Marked anti-tumor effects were demonstrated in the AEC-treated CT26 cells. In the *in vivo* syngeneic model, the AEC treatment decreased the volume and weight of CT26 tumors, and expanded the necrotic region in the hematoxylin and eosin stained tumor sections. The inhibitory effects of AEC on tumor growth were reflected by the increased level of apoptotic proteins, inhibition of cell proliferation, suppression of metastasis ability and increase in tumor-suppressing activity in CT26 tumor-bearing BALB/cKorl syngeneic mice. The potential function of phlorotannin (PT), one of the primary active compounds in AEC, was demonstrated by the increased cytotoxicity, apoptosis and suppression of cell proliferation in PT-treated CT26 cells. Overall, the results of the present study provide novel scientific evidence that AEC can suppress the growth of CT26 colon cancer by activating apoptosis, suppressing cell proliferation, inhibiting cell migration and enhancing the tumor-suppressing activity.

Correspondence to: Professor Dae Youn Hwang, Department of Biomaterials Science (BK21 FOUR Program), College of Natural Resources & Life Science/Life and Industry Convergence Research Institute/Laboratory Animal Resources Center, Pusan National University, 1268-50 Samnangjin-ro, Samnangjin-eup, Miryang, Gyeongsangnam 50463, Republic of Korea
E-mail: dyhwang@pusan.ac.kr

Key words: *Ecklonia cava*, CT26 colon cancer, tumor, apoptosis, proliferation, migration

Introduction

Ecklonia cava (*E. cava*) is a perennial brown alga found widely along the coastal regions of Korea and Japan that has been used traditionally as a food and food with medicinal properties (1). *E. cava* contains numerous natural, bioactive compounds and their various derivatives, including the major compound, phlorotannins (PT), as well as peptides, carotenoids and sulfated polysaccharides (2,3). Previous studies have reported the beneficial effects of *E. cava* extract, such as antioxidant properties (4,5), anti-human immunodeficiency virus type-1 activity (6), stimulatory effects for apoptosis (7), inhibitory effects for angiotensin 1-converting enzyme (8), anti-inflammatory effects (9) and anti-diabetic effects (10).

The potential for anti-tumor drugs from *E. cava* has been previously assessed; however, most studies used only *E. cava*-derived compounds, such as dieckol (11), dioxinodehydroeckol (7) and 6,6'-bieckol (12). Among these *E. cava*-derived compounds, the anti-tumor activity of dieckol has been widely reported in several cells and animal models (11-16). Dieckol inhibited the expression of vascular endothelial growth factor (VEGF) protein and matrix metallopeptidase (MMP)-9, and suppressed cell movement as well as stimulated tissue inhibitor of metalloproteinases (TIMP)-1/2 in MCF-7 cells (13). Moreover, dieckol was reported to have had anti-tumor effects, including apoptosis activation, tumor growth suppression, increased reactive oxygen species (ROS) production and suppression of the Akt/p38 signaling pathway in ovarian cancer cells and a xenograft model (11). Similar suppressive effects on invasion and angiogenesis were reported in an N-nitrosodiethylamine-induced hepatocarcinogenesis model after dieckol treatment (14). Furthermore, dioxinodehydroeckol derived from *E. cava* was reported to have had inhibitory effects against the proliferation of MCF-7 cells via regulation of the nuclear factor (NF)-κB signaling

pathway (7). Another compound, 6,6'-bieckol, was reported to have inhibited the expression of MMP-2/9, cell migration and the NF-κB signaling pathway (12). Certain extracts and complexes derived from *E. cava* have been reported to have had similar anti-tumor effects in numerous cancer cells. For example, the bioactive compounds extracted from *E. cava* using carbohydrase hydrolysis suppressed the growth and proliferation of CT26 colon cancer cells (15). The complex sulfated polysaccharides derived from *E. cava* was also reported to have had anti-tumor effects on cell growth, apoptotic body formation, caspase (Cas)-9/poly (ADP-ribose) polymerase expression and the Bax/Bcl-2 signaling pathway (16). However, to the best of our knowledge, there have been no reports on the anti-tumor effects and mechanism of the aqueous extract of *E. cava* (AEC) against colon cancer.

The present study was intended to be assess the anti-tumor effects and molecular mechanism of AEC in CT26 cells and BALB/cKorl syngeneic mice with a CT26 tumor.

Materials and methods

Preparation of AEC and PT. AEC samples were prepared as described previously (17) with slight modification. Firstly, dried samples of *E. cava* were purchased from Para Jeju Co. Ltd., and were deposited as voucher specimens (accession no. WPC-19-001) at the Functional Materials Bank of the Wellbeing RIS Center at Pusan National University (Pusan, Korea). After extraction using mixture of AEC samples and distilled dH_2O solvent (1:15 ratio), the lyophilized AEC pellets were harvested in an N-1100 series rotary evaporator (Tokyo Rikakikai Co., Ltd.).

PT was extracted according to the method previously described by Lee *et al* (18) with slight modification. The dried *E. cava* powder (30 g) was mixed with 70% ethanol (300 ml; v/v) and the extract was then collected by shaking for 12 h at 37˚C. After repeating the extraction process three times, the total extracted solution was filtered using a membrane with 8 mm pore size and then evaporated at 40˚C. These extracts were dissolved in dH_2O, and sequentially fractionated using n-hexane, chloroform and ethyl acetate. Finally, ethyl acetate fraction was evaporated at 40˚C to remove the solvent, and used as the PT-rich sample, as reported previously (18,19).

Determination of four bioactive compounds in AEC. Total phenolic content (TPC) concentration was assessed using the Folin-Denis method, as previously described (20). Briefly, after consistently mixing the AEC solution, Folin-Ciocalteu reagent and 10% Na_2CO_3 solution for 1 h at 37˚C, the absorbance of each well was measured at 725 nm. The concentration of TPC in AEC was estimated using a standard calibration curve for caffeic acid (MilliporeSigma) because it is considered as one of the major phenolic acids. Total flavonoid content (TFC) was assessed using the Davis method as previously described (21). Briefly, after constantly mixing AEC solution, 1 N $NaNO_2$ and 90% $C_4H_{10}O_3$ for 1 h at 37˚C, the absorbance of each well was measured at 420 nm. The concentration of TFC in AEC was estimated using a standard calibration curve for naringin (MiliporeSigma) because naringin and its aglycone naringenin belong to this series of flavonoids. Total condensed tannin content (TTC) was assessed using the Vanillin method as previously described (22). Briefly. the concentration of TTC in AEC was estimated based on a standard calibration curve for a purified (+)-catechin hydrate standard (MilliporeSigma) because catechin has all the characteristics of condensed tannin. Finally, the concentration of total PT content (TPTC) was determined using the Folin-Ciocalteu method as described previously (23). The concentration of TPTC in AEC was estimated using a standard calibration curve for phloroglucinol (MilliporeSigma) because PT is a complex polymer of phloroglucinol, which is a specific compound found in brown algae. TPC, TFC, TTC and TPTC in AEC were presented as caffeic acid, naringin, catechin hydrate and phloroglucinol equivalents (mg) of AEC, respectively.

Analysis for free radical scavenging activity. The scavenging activity of 2,2-diphenyl-1-picrylhydrazyl (DPPH) radicals was analyzed as previously described by Go *et al* (23). Briefly, after incubation of AEC and 0.1 mM DPPH solution (MilliporeSigma) for 30 min at room temperature, the absorbance of each well was measured at 517 nm using a VersaMax plate reader (Molecular Devices, LLC). AEC scavenging activity for DPPH radicals activity was presented as the half-maximal inhibitory concentration (IC_{50}) based on the percentage decrease in absorbance relative to the control group.

Liquid chromatography-mass spectrometry (LC-MS) analysis. Bioactive compounds in AEC were assessed using an Agilent 1290 Infinity high-performance liquid chromatography (HPLC) system (Agilent Technologies Deutschland GmbH), coupled with a hybrid quadrupole time-of-flight mass spectrometer (Agilent Technologies Deutschland GmbH). Detailed conditions and the column for LC-MS analysis as well as data analysis were performed as described previously (17). Briefly, LC-MS signals were detected on a mass spectrometer operating in the positive ionization mode. A HSS T3 Column (2.1x100 mm, 1.8 μm; Waters Corporation) was used for chromatographic separation under the following conditions: 0.2 ml/min in flow rate, 10 μl of injection volume, water as mobile phase A, and 100% acetonitrile as mobile phase B. For MS detection, the operating parameters were as follows: Gas temperature, 300˚C; gas flow, 9 l/min; nebulizer pressure, 45 psi; sheath temperature, 350˚C; sheath gas flow, 11 l/min; VCap, 4,000 V; fragmentor voltage, 175 V. All the acquisition and analysis of data were controlled by MassHunter software (version B. 0600, Agilent Technologies).

Cell culture and viability assay. Murine colorectal carcinoma CT26 cells from a BALB/c mouse, were used to evaluate the anti-tumor effects of AEC because they successfully form solid tumors and metastasize into other organs in BALB/c or immunocompromised mice. A HCT116 cancer cell line from the colon tissue of an adult male with colon cancer, was used to evaluate whether anti-tumor effects of AEC in colon cancer cells of murine were similar in human colon cancer cells. Fibroblast Detroit 551 cells from the skin of a normal human embryo, were used to assess whether AEC was toxic to normal cells. These three cell lines were purchased from the American Type Culture Collection. The medium with 10% fetal bovine serum (Welgene, Inc.) were prepared appropriately for each cell line; a Roswell Park Memorial Institute 1640 Medium (Welgene, Inc.) for CT26 cells, McCoy's 5a Medium (Welgene, Inc.) for HCT116 cells and

Minimum Essential Medium Eagle (Welgene, Inc.) for Detroit 551. The viability of the CT26, HCT116 and Detroit 551 cells was determined after treatment with AEC using the tetrazolium compound, MTT (MilliporeSigma) as described previously (21). The optimal concentration of AEC was determined based on the anti-tumor activity of *E. cava* extract in human breast cancer cells (21) and the dose-response curve of AEC in CT26, HCT116 and Detroit 551 cell lines (Fig. S1A, B and C). Cells at 70-80% confluence were treated with either the dH_2O (Vehicle treated group, Vehicle) or pretreated with 5 μg/ml Cisplatin (Cis treated group, Cis), 600 (Low dose AEC, LoAEC treated group), 800 (Medium dose AEC, MiAEC treated group) or 1,000 μg/ml (High dose AEC, HiAEC treated group) AEC for 24 h at 37˚C. In the case of the PT treatment, the CT26 cells were treated with 100 (Low dose PT, LoPT treated group), 150 (Medium dose PT, MiPT treated group) or 200 μg/ml (High dose PT, HiPT treated group) PT for 24 h at 37˚C. The optimal dosage of PT was determined based on previous results which reported IC_{50} from 56.3 to 219 μg/ml in MKN-28, Caco-2 and HT-29 cells (24) and the dose-response curve of PT in CT26 cell lines (Fig. S1D). After incubation for 24 h, 200 μl of fresh medium and 50 μl of MTT solution (2 mg/ml in 1x PBS) were added to each well, with the supernatants discarded. After incubation at 37˚C for 4 h, the formazan precipitate in each well was dissolved entirely in dimethyl sulfoxide (DMSO, Duchefa Biochemie, B.V.), and the absorbance was read at 570 nm using a Vmax plate reader (Molecular Devices LLC). Before the detection of the level of the formazan precipitate, the morphological changes of cells were observed using an optical microscope (Leica Microsystems GmbH) at a 400x magnification.

Furthermore, the cell viability assessed using the MTT assay was also evaluated based on the quantification of the ATP present, because ATP concentration indicates the presence of metabolically active cells, using CellTiter-Glo assay kit (Promega Corporation) according to the manufacturer's protocol. After mixing cell culture medium and CellTiter-Glo® Reagent, the luminescent signal from each well was measured under an GloMax® 20/20 Luminometer (Promega Corporation) and ATP concentration were determined using an ATP standard curve.

Immunofluorescence (IF) staining analysis of cells. AEC treated CT26 cells were fixed using 4% formaldehyde for 1 h at room temperature and permeabilized using 1% Triton X-100, were incubated with 0.5% bovine serum albumin (BSA) for 1 h at room temperature and then Ki67/MKI67 primary antibodies (1:20; cat. no. NB500-170s; Novus Biologicals, LLC) for 12 h at 4˚C. The cells were subsequently incubated with Alexa Fluor 488 goat anti-rabbit IgG (1:100; cat. no. A11008; Thermo Fisher Scientific, Inc.) secondary antibodies for 1 h at room temperature. Ki67 positive cells in CT26 cells were detected based on the green fluorescence intensity using an EVOS™ M5000 Imaging System (Thermo Fisher Scientific, Inc.). Their number was counted in the total area of the field of view (67,500 μm^2) for each well of CT26 cells using the Imaging System.

Analysis of apoptotic cells using fluorescence-activated cell sorting. The number of apoptotic cells was analyzed using a Muse™ Annexin V and Dead Cell Kit (MilliporeSigma). Briefly, the wells containing the CT26 cells were divided into six groups (No, Vehicle, Cis, LoAEC, MiAEC, and HiAEC) for the AEC experiment. After being treated with aforementioned concentrations of AEC and Cis for 24 h at 37˚C, the cells were treated with annexin V and 7-aminoactinomycin D (7-AAD) for 20 min at room temperature. The distribution of the stained cells were analyzed using a Muse™ Cell Analyzer (MilliporeSigma). After gating analyzed data based on the cell size, cells were classified into four groups: non-apoptotic cells, early apoptotic cells, late apoptotic cells and primarily nuclear debris as described previously (21).

Western blotting analyses. Total protein was collected from the CT26 cells and CT26 tumors of BALB/cKorl syngeneic mice using the Pro-Prep Protein Extraction Solution (Intron Biotechnology, Inc.). The tissue homogenates were prepared from two to three solid tumors per group based on the results of the measurement of weight and hematoxylin and eosin (H&E) staining analysis. After homogenizing the tumor, total proteins were harvested, and their concentration was determined using a SMART™ Bicinchoninic Acid Protein assay kit (Thermo Fisher Scientific, Inc.). Total proteins (30 μg/lane) were separated on 4-20% gradient SDS-PAGE for 2 h at 100 V, and they were subsequently transferred to nitrocellulose blotting membranes with a 0.45 μm pore size for 2 h at 40 V. Proteins bounded on nitrocellulose membranes were incubated with primary antibodies (Table SI) overnight at 4˚C. After removing the non-specifically bound antibodies using washing buffer (137 mM NaCl, 2.7 mM KCl, 10 mM Na_2HPO_4 and 0.05% Tween 20), the membranes were incubated with HRP-conjugated goat anti-rabbit IgG (1:1,000; cat. no. HS101; Transgene Biotech Co., Ltd.). The intensity of each protein was analyzed using a Chemiluminescence Reagent (Pfizer, Inc.) using the FluorChem® FC2 imaging system (ProteinSimple). Finally, the density of each protein was quantified using AlphaView (Version 3.2.2, Cell Biosciences, Inc.).

Animal experiments. The protocol for experimental animal study was reviewed and approved by the Pusan National University Institutional Animal Care and Use Committee (approval no. PNU-2020-0108). To ensure the reliability of the data from the animal study, the total number of animals was determined as 35 using G-POWER 3.1.9.7 (Heinrich-Heine-Universität Düsseldorf, Germany) with the α probability of 0.05, effect size of 0.8 and a power of 0.80. Seven week old male BALB/cKorl mice (n=35) were supplied by the National Institute of Food and Drug Safety Evaluation (Cheongju, Korea) of the Korea Food and Drug Administration (KFDA). The BALB/cKorl syngeneic mice were bred at the Pusan National University-Laboratory Animal Resources Center, which is accredited by the KFDA (accredited unit 000231) and The Association for Assessment and Accreditation of Laboratory Animal Care International (accredited unit 001525). Mice were provided, *ad libitum*, with filtered tap water and a standard irradiated chow diet (Samtako Co., Ltd.). All mice were maintained in a specific pathogen-free state, with a strictly regulated 12 h light/dark cycle, and constant temperature (22±2˚C) and relative humidity (50±10%).

The anti-tumor activity of AEC was evaluated in the BALB/cKorl syngeneic mice for a 37 day period using a slight modification of methods reported previously (25,26). Briefly,

$4x10^5$ CT26 cells were injected subcutaneously into the back region of BALB/cKorl mice on day 1. CT26 tumor-bearing BALB/cKorl syngeneic mice (n=35) were divided randomly into one of five groups (n=7/group). The first group (Vehicle treated group, n=7) was orally administrated the same volume (200 μl) of 1x PBS every day for five weeks. The second group (Cis treated group, n=7) was injected intraperitoneally with Cis (4 mg/kg) every two days from day 26 to day 37, because long-term administration of Cis causes serious toxicity and can lead to death (27). The other three groups were administered a low (250 mg/kg; LoAEC treated group, n=7), medium (500 mg/kg; MiAEC treated group, n=7) or high concentration of AEC (1,000 mg/kg; HiAEC treated group, n=7) orally every day for 37 days. The health and behavior of all mice were monitored every day before treatment was administrated. No animals died during the experimental period. Bedding was abundantly provided as special housing condition to help animals maintain their body temperature. Furthermore, humane endpoints were set when the tumor exceeded 4,400 mm^3 in volume (28) and when body weight of mice decreased >20% within 1-2 weeks, to prevent pain or distress of mice. At 24 h after the final treatment, all BALB/cKorl syngeneic mice were euthanized by a trained researchers using an appropriate chamber with gas regulator and CO_2 gas with a minimum purity of 99.0% based on the AVMA Guidelines for the Euthanasia of Animals. A cage containing animals was placed in the chamber and CO_2 gas of 99.0% was introduced into chamber without pre-charging, with a fill rate of ~50% of the chamber volume per minute. The death of mice were confirmed by ascertaining cardiac and respiratory arrest, or dilated pupils and fixed body. The solid tumors were then collected from all euthanized BALB/cKorl syngeneic mice (Fig. S2).

Determination of tumor volume and weight. The size of CT26 tumors was measured daily during oral administration of AEC (from day 1 to 36). The tumor volume was determined based on the measurement results for length and width of the tumors using the following formula: Tumor volume (mm^3)=(length x $width^2$)/2. Images of each tumor formed in the mice were taken after the last administration using a micro computed tomography (microCT) scanner (Nano Focus Ray Co., Ltd.). The tumor volume in the microCT image was quantified using ImageJ 1.52a (National Institutes of Health). The weight of each tumor was assessed, once excised, using an electrical balance in duplicate.

Histopathological analysis. The CT26 solid tumor collected from the BALB/cKorl syngeneic mice model was fixed in a 10% formalin solution for 48 h at room temperature, and then the middle region of solid tumor was embedded into paraffin block. Following sectioning the tumor block into 4 mm thick slices, these section were stained with a H&E solution (Sigma-Aldrich; Merck KGaA) for 4 min 15 sec at room temperature. After optical microscopic examination of the tumor sections at 400x magnification, the tumor type and pathological features were characterized by Professor Beum Seok Han at Hoseo University (Asana, Korea). The necrotic areas on the H&E stained tumor sections were measured and quantified, as described previously (29).

IF staining analysis of tissue. The aforementioned tissue sections of CT26 solid tumor (two to three samples per group) were deparaffinized with xylene, rehydrated using a decreasing EtOH series, and then washed three times with dH_2O for 5 min at room temperature. These sections were blocked using 10% goat serum (Vector Laboratories, Inc.; Maravai LifeSciences) in 1x PBS solution for 30 min at room temperature. The tissue slides were incubated with anti-Ki67/MKI67 (1:100; cat. no. NB500-170s; Novus Biologicals) primary antibodies for 12 h at 4˚C, and then with goat fluorescein isothiocyanate (FITC)-labeled anti-rabbit IgG secondary antibodies (1:100; cat. no. 65-6111; Thermo Fisher Scientific, Inc.) for 45 min at room temperature. Finally, Ki67 positive cells in tumor sections were detected based on the green fluorescence intensity using an EVOS™ M5000 Imaging System (Thermo Fisher Scientific, Inc.). Their number was counted in the total area of the field of view (67,500 mm^2) for each CT26 tumor section using the Imaging System.

Whole blood and serum analysis. After anesthesia with an intraperitoneal injection of anesthetic mixture (4:1 ratio) containing of 40 mg/kg Alfaxan (Jurox Pty Limited) and 10 mg/kg Rompun (Bayer-Korea, Ltd.) based on previous report (30), the abdominal region of BALB/cKorl syngeneic mice were opened by sterile scissors. Before opening, adequate anesthesia of mice was ensured by testing the pedal withdrawal reflex (clasping one's toes with tweezers) and lacking the eye blink reflex. The whole blood sample was collected from the abdominal veins using 1 ml syringe (26 SWG), and subsequentially the mice were terminated by cervical dislocation. The levels of 12 key factors were analyzed by an automated cell counter (Beckman-Coulter, Inc.) using the Vetscan HM5 Reagents Pack (cat. no. 89126-098; Abaxis, Inc.; Zoetis Services LLC) according to the manufacturer's protocols. The levels of white blood cells, red blood cells, hemoglobin, hematocrit, mean corpuscular volume, mean corpuscular hemoglobin, mean corpuscular hemoglobin concentration, corpuscular hemoglobin concentration mean, corpuscular hemoglobin content, hemoglobin concentration distribution width, platelets and mean platelet volume were measured in duplicate for each sample.

Serum samples were obtained from whole blood sample after centrifugation at 1,500 x g for 10 min at 4˚C. The concentrations of 5 serum biochemical components were analyzed using a Hitachi 747 automatic serum analyzer (Hitachi, Ltd.). All analysis were performed in duplicate using fresh samples.

Statistical analysis. One-way ANOVA (SPSS for Windows, Release 10.10, IBM Corp.) was used to assess statistical significance between the treatment groups, and followed by Tukey's post-hoc test for multiple comparisons. $P<0.05$ was considered to indicate a statistically significant difference, and all values were presented as the mean ± standard deviation (SD).

Results

Composition and antioxidative activity of AEC. To evaluate the potential antioxidative activity of AEC, the main phytochemical classes and DPPH radical scavenging activity of AEC were analyzed. Among the three phytochemicals, TPC

A

Category	Concentration (mg/g)
TPC	108.05±4.50
TTC	29.19±0.13
TFC	6.88±0.45
TPTC	2.60±0.06

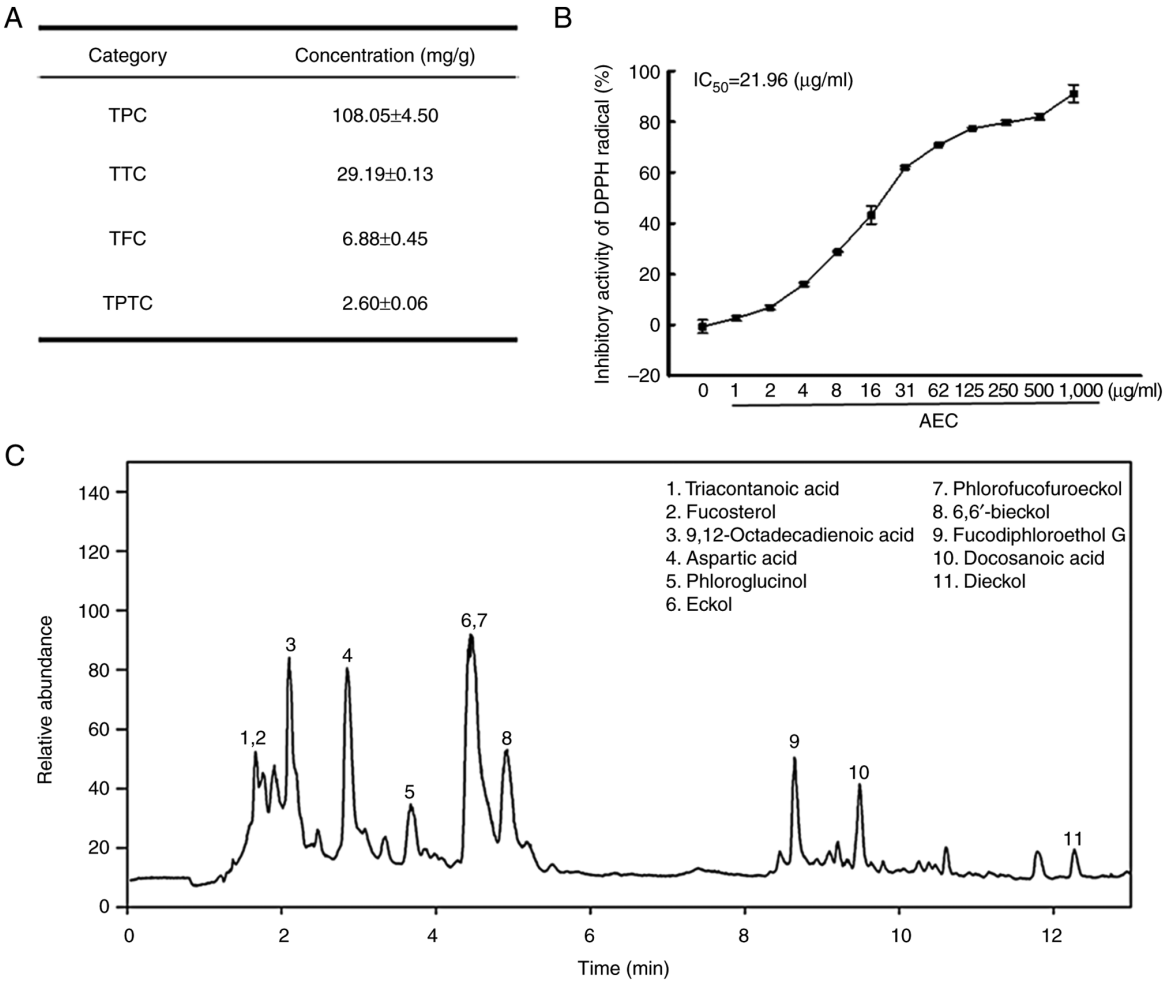

Figure 1. Major phytochemical composition and DPPH radical scavenging activity of AEC. (A) TPC, TTC, TFC and TPTC levels in AEC were analyzed as described in the Materials and methods. (B) The scavenging activity for DPPH radicals was measured in solutions containing 0.1 mM DPPH and twelve different concentrations (0-1,000 μg/ml) of AEC. Two samples for each assay were analyzed twice by DPPH analysis. The data for above results are presented as the mean ± SD. (C) LC-MS analysis of AEC. Eleven bioactive components including triacontanoic acid, fucosterol, 9,12-octadecadienoic acid, aspartic acid, phloroglucinol, eckol, phlorofucofuroeckol, 6,6'-bieckol, fucodiphloroethanol G, docosanoic acid and dieckol were detected as different peaks in the chromatogram. DPPH, 2,2-diphenyl-1-picrylhydrazyl; AEC, aqueous extract of *Ecklonia cava*; TPC, total phenolic content; TTC, total condensed tannin contents; TFC, total flavonoid content; TPTC, total PT content; IC_{50}, half maximal inhibitory concentration.

was detected at the highest concentrations (108.05 mg/g), whereas the TTC and TFC concentrations were relatively low (29.19 and 6.88 mg/g, respectively). Furthermore, the concentration of TPTC was 2.60 mg/g (Fig. 1A). In addition, the scavenging activity of AEC against the DPPH radical increased markedly in a dose-dependent manner, with an IC_{50} value of 21.96 μg/ml (Fig. 1B). These concentrations of phytochemicals and DPPH radical scavenging activity were similar to those reported elsewhere (31). Furthermore, eleven active components, including 9,12-octadecadienoic acid (32), aspartic acid (33), eckol (34), phlorofucofuroeckol (35) and dieckol (36), were identified and characterized using LC-MS analyses (Figs. 1C and S3). Among them, six compounds, including phloroglucinol, eckol, 6,6'-bieckol, phlorofucofuroeckol, fucodiphloroethol G and dieckol, belonged to PT, which contains numerous separate compounds, and is classified into four subclasses: the fuhalols and phlorethols group, the fucols group, the fucophlorethols group and the eckols group (5,35,36). Therefore, these results indicated that AEC had potential antioxidant activity.

Cytotoxicity of AEC against CT26 cells. The viability of CT26 cells was determined using an MTT assay, cell morphological analysis and ATP concentration assay after exposure to three different AEC concentrations for 24 h to determine if exposure to AEC induced the cytotoxicity of CT26, HCT116 and Detroit 551 cells. The viability of CT26 cells in MTT assay was decreased significantly in a dose-dependent manner, and the highest cytotoxicity was demonstrated in the HiAEC treated group (Fig. 2A). The results detected using the MTT assay were reflected in the morphological changes seen in CT26 cells (Fig. 2A) and indicated that AEC exerted significant cytotoxicity on CT26 cells at concentrations <1,000 μg/ml. Furthermore, the number of cells stained with Ki67 proteins, a marker for cell proliferation, was significantly decreased after the AEC treatment compared with the No or Vehicle treatment groups (Fig. 2B). Furthermore, the effects of AEC on the cell viability assessed using the MTT assay were also demonstrated in the cell viability assessed based on the concentration of ATP although there are differences in dose-dependent responses (Fig. 2C). Moreover, the cytotoxicity of AEC was similarly

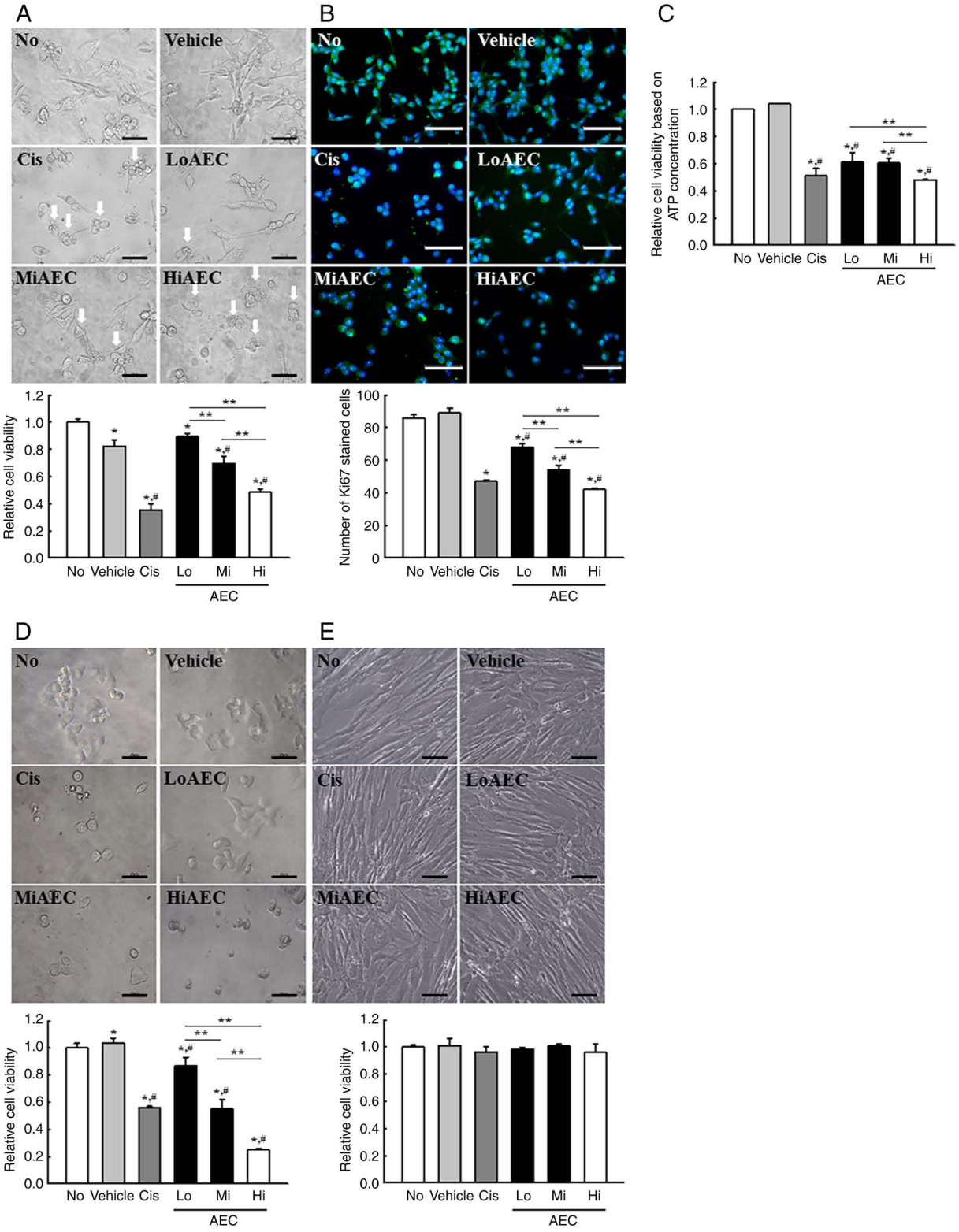

Figure 2. Cytotoxicity and IF staining of AEC-treated CT26 cells. (A) Relative cell viability of AEC in CT26 cells assessed using an MTT assay based on the optical density of the solubilized formazan. After incubating CT26 cells with AEC for 24 h, the morphology of the CT26 cells was observed using an inverted microscope at 400x magnification. Arrows indicated abnormal cells. The MTT assay was performed on two to three wells per group, and the optical density was measured twice for each well. (B) Protein expression level of Ki67. The preparation of Ki67 stained samples was performed on two to three wells per group, and Ki67 positive cells was counted in two fields of view (67,500 mm^2) in each well. (C) Relative cell viability of AEC in CT26 cells using CellTiter-Glo luminescent assay. After incubating CT26 cells with AEC for 24 h, the viability of cells based on the ATP concentration were assessed using the CellTiter-Glo® Assay kit. (D) Relative cell viability of AEC in HCT116 cells was assessed using the MTT assay based on the optical density of the solubilized formazan. After incubating HCT116 cells with AEC for 24 h, cell viability and morphology were analyzed in the same way as CT26 cells. (E) Relative cell viability of AEC in Detroit 551 cells was assessed using the MTT assay based on the optical density of the solubilized formazan. After incubating Detroit 551 cells with AEC for 24 h, cell viability and morphology were analyzed in the same way as CT26 cells. Scale bar=50 μm. The relative level was calculated as a relative percentage considering the Vehicle group as 100%. Data was presented as the mean ± SD. *P<0.05 vs. No group. $^{\#}$P<0.05 vs. Vehicle group. **P<0.05 vs. between three AEC treated group. IF, immunofluorescence; AEC, aqueous extract of *Ecklonia cava*; No, untreated; Cis, cisplatin; Lo, low concentration; Mi, middle concentration; Hi, high concentration.

demonstrated in HCT116 cells which are colorectal carcinoma cells derived from an adult male (Fig. 2D). However, AEC did not cause any toxicity in Detroit 551 normal fibroblast cell line derived from a skin tissues of human fetus (Fig. 2E). These results indicated that AEC exerts significant cytotoxicity in CT26 and HCT116 colon cancer cells at concentrations <1,000 μg/ml without any significant toxicity to normal skin fibroblast cells.

Effects of AEC on the apoptosis-associated response of CT26 cells. Experiments in CT26 cells were performed to evaluate if the cytotoxicity effects of AEC were related to changes in the apoptosis-associated response. The number of live and apoptotic CT26 cells were assessed using Annexin V/PI staining analysis, and the protein expression levels of the mitogen-activated protein kinases (MAPK) signaling pathway members and apoptosis regulatory proteins were assessed using specific antibodies. After treatment with only HiAEC, the number of apoptotic cells was significantly increased, with a concomitant decrease in the number of live cells, compared with the Vehicle group (Fig. 3A). The increase in the number of apoptotic cells was reflected by the protein expression levels of the proteins related to the Bax/Bcl-2 and MAPK signaling pathways. The AEC-treated group demonstrated significantly enhanced p-c-Jun N-terminal kinase (p-JNK), p-extracellular signal-regulated kinase (p-ERK), and p-p38 protein expression levels compared with the Vehicle group, even though the increase rate of phosphorylation of each protein was varied (Fig. 3B). A similar response was demonstrated in the relative protein expression levels of Cleaved Cas-3/Cas-3 and Bax/Bcl-2, which were increased significantly in the LoAEC, MiAEC and HiAEC treated groups compared with the Vehicle group (Fig. 3B). These results indicated that the cytotoxic effects of AEC may be tightly linked to the promotion of the apoptosis-related response and activation of the MAPK and Bax/Bcl-2 signaling pathways.

Inhibitory effect of AEC on the growth of CT26 tumors in BALB/cKorl syngeneic mice. The present study evaluated whether the anti-tumor activity of AEC in CT26 colon cancer cells could be reproduced entirely in the BALB/cKorl syngeneic mice with CT26 tumors. The changes in the volume and histopathological structure of the tumor were analyzed in CT26 tumors of BALB/cKorl syngeneic mice treated with three different doses of AEC for five weeks. The volume of the tumor markedly decreased in the AEC treated groups compared with the Vehicle group, and a significant reduction in the weight of them was demonstrated in the MiAEC treated group compared with the Vehicle group, but not HiAEC treated group (Fig. 4A and B). A similar effect on the tumor volume was also demonstrated in actual and microCT imaging (Fig. 4C). Furthermore, few spots containing cell necrosis were detected in the H&E stained sections of CT26 tumors in the Vehicle treated group. The necrotic region of these spots was markedly expanded after the AEC treatment compared with the Vehicle treated group. Certain pathological alterations, including hemorrhage, cyst formation and angiogenesis, were observed in the AEC treated tumors of BALB/cKorl syngeneic mice (Fig. 5A and B). By contrast, no significant differences in the toxicity parameters, including body, kidney and liver weight, cell composition of the blood, metabolites of the serum, and the histopathological structure of the liver and kidney were demonstrated between the Vehicle and AEC treated groups (Figs. S4-7). These results indicated that AEC treatment could inhibit the growth of CT26 tumors in BALB/cKorl syngeneic mice without significant toxicity.

Effects of AEC on the cell proliferation in CT26 tumors of BALB/cKorl syngeneic mice. The tissue distribution of Ki67 and proliferating cell nuclear antigen (PCNA) proteins were evaluated using specific antibodies in AEC treated tumors of BALB/cKorl syngeneic mice to evaluate if the inhibitory activity of AEC on CT26 tumor growth was accompanied by a change in cell proliferation ability. The fluorescent intensity for the Ki67 proteins significantly decreased with increasing AEC dose in CT26 tumors of BALB/cKorl syngeneic mice (Fig. 6A). A similar pattern was observed with a significant decrease of the protein expression level of PCNA (Fig. 6B). These results indicated that the inhibitory activity of AEC on CT26 tumor growth could be linked to the suppression of tumor cell proliferation in BALB/cKorl syngeneic mice.

Effects of AEC on the apoptosis-associated response in CT26 tumors of BALB/cKorl syngeneic mice. Alterations to the protein expression levels of the major proteins within the MAPK and Bax/Bcl-2 signaling pathways were assessed in the AEC treated tumors of BALB/cKorl syngeneic mice to evaluate if the inhibitory effects of AEC on CT26 tumor growth were accompanied by changes in the apoptosis-associated response. In the MAPK signaling pathway, the phosphorylation of ERK, JNK and p38 increased significantly in all AEC treated groups compared with the Vehicle treated group (Fig. 7A). Furthermore, a similar pattern of increase was demonstrated in the Bax/Bcl-2 signaling pathway, where the protein expression levels of Bax/Bcl-2 and Cleaved Cas-3 proteins were increased significantly in the AEC treated group compared with the Vehicle group (Fig. 7B). These results indicated that the inhibitory effects of AEC on CT26 tumor growth may be associated with the enhanced phosphorylation of several members of the MAPK signaling pathway and the critical proteins in the Bax/Bcl-2 signaling pathway.

Effects of AEC on the migration ability in CT26 tumors of BALB/cKorl syngeneic mice. The alteration of the protein expression levels of key proteins in the myosin light chain (MLC)/focal adhesion kinase (FAK)/Akt signaling pathway were assessed in the AEC treated tumors of BALB/cKorl syngeneic mice to evaluate if the inhibitory activity of AEC on the CT26 tumor growth were accompanied by suppression of the migration ability. Protein expression levels of the vascular endothelial growth factor A (VEGFA), matrix metallopeptidase (MMP)2, and MMP9 proteins were significantly lower in the AEC treated group compared with the Vehicle treated group, even though their rate was varied (Fig. 8A). Furthermore, a similar decreasing pattern was demonstrated in the regulation of the MLC/FAK/Akt signaling pathway proteins. In the MLC/FAK signaling pathway, the phosphorylation levels of FAK and MLC decreased markedly in the AEC treated groups compared with the Vehicle treated group (Fig. 8B). In the phosphoinositide 3-kinases (PI3K)/Akt

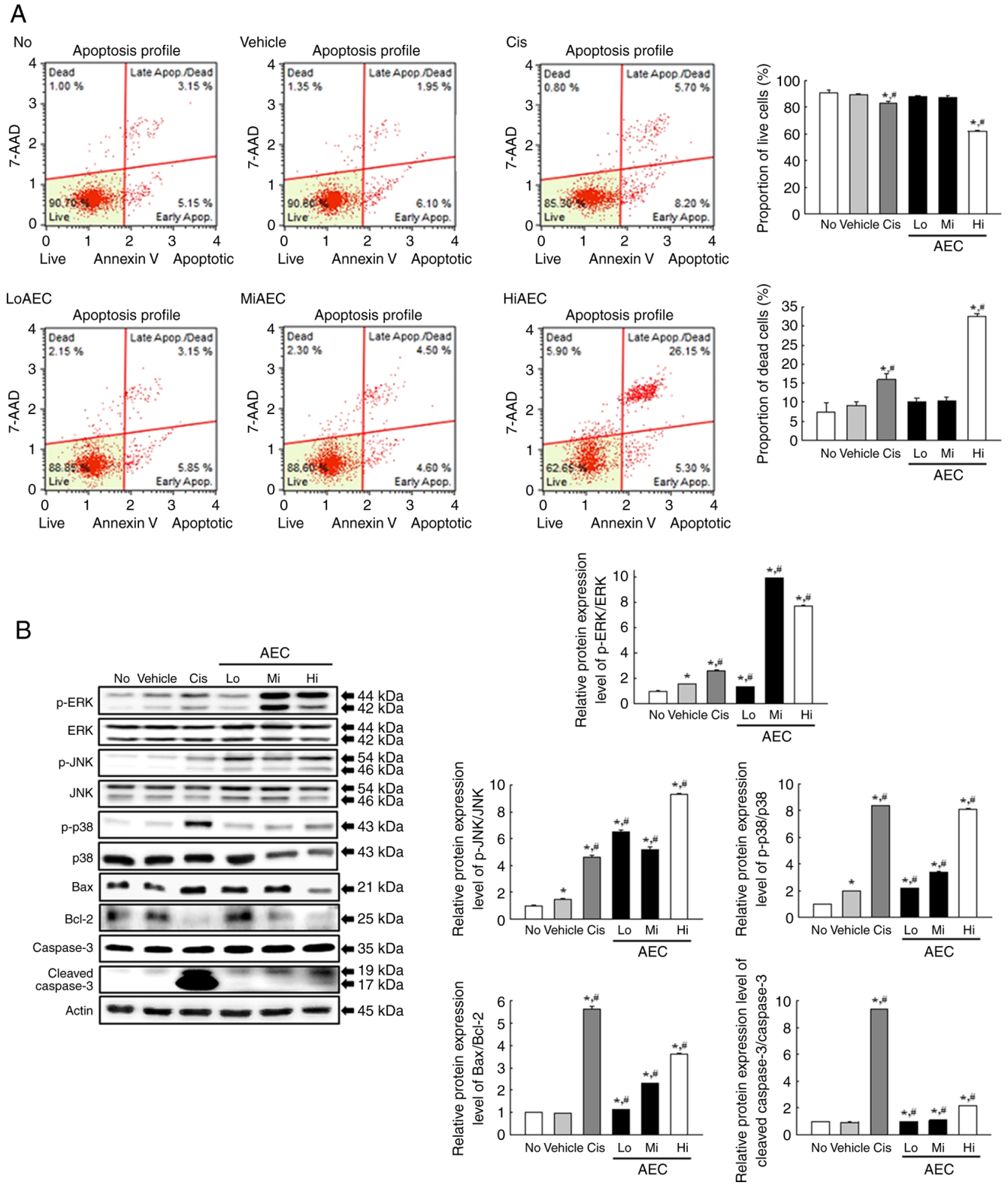

Figure 3. Apoptotic cells and related protein analysis of AEC treated CT26 cells. (A) Apoptosis analysis of CT26 cells. After treatment with AEC for 24 h, the number of CT26 cells was analyzed in each group stained with annexin V and 7-AAD. Annexin V and 7-AAD staining were performed on two to three wells per group, and the dead cells and live cells were counted twice for each well. (B) MAPK and Bax/Bcl-2 protein analysis. After treatment with AEC for 24 h, the band density for specific protein was analyzed using densitometry. The preparation of the cell homogenates was performed on two to three dishes per group, and western blotting was analyzed twice for each sample. The level of each protein was normalized to β-actin. The data was presented as the mean ± SD. *P<0.05 vs. No group. #P<0.05 vs. Vehicle group. AEC, aqueous extract of *Ecklonia cava*; No, untreated; Cis, cisplatin; Lo, low concentration; Mi, middle concentration; Hi, high concentration; p, phosphorylated.

signaling pathway, the phosphorylation levels of PI3K and Akt proteins were significantly decreased in the AEC treated group compared with the Vehicle group (Fig. 8C). Therefore, the inhibitory effects of AEC on CT26 tumor growth may

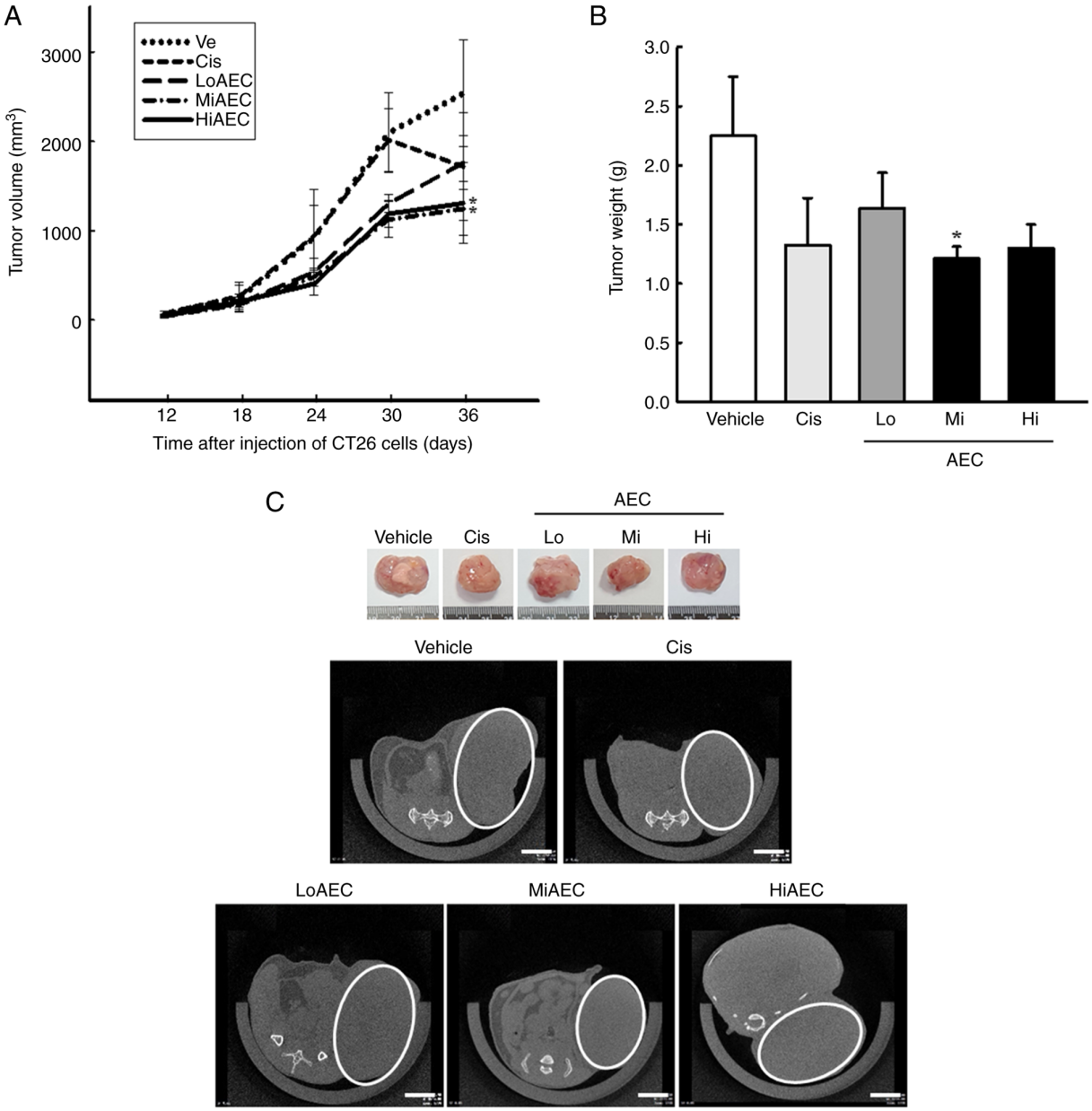

Figure 4. Growth of CT26 tumors in BALB/cKorl syngeneic mice. (A) Volume of CT26-induced tumor. The solid tumor size was presented only from day 12 to 36 because they were not palpable before this. (B) Weight of the CT26 tumors. On day 36, CT26 tumors were isolated from the subcutaneous region of the syngeneic model. (C) Tumor image and microCT. The photographic images of the CT26 tumor are presented at the top. After anesthetizing each mouse, an image of all tumors was taken by microCT. Scale bar=5 mm. The weight and volume were measured twice for each mice. The data was presented as the mean ± SD. *P<0.05 vs. Vehicle group. AEC, aqueous extract of *Ecklonia cava*; Cis, cisplatin; Lo, low concentration; Mi, middle concentration; Hi, high concentration.

be associated with suppression of the migration ability of tumor cells through alternative control of the MLC/FAK/Akt signaling pathway.

Effects of AEC on the tumor suppressing activity in CT26 tumors of BALB/cKorl syngeneic mice. Whether the inhibitory activity of AEC on CT26 tumor growth was accompanied by changes in the protein expression level of tumor suppression-related proteins and the NF-κB signaling pathway was evaluated. Changes in the protein expression levels of the tumor suppression-related and the NF-κB signaling pathway proteins were evaluated in the AEC treated tumors of BALB/cKorl syngeneic mice. The protein expression levels of p53, mouse double minute 2 (MDM2) and p27 increased markedly in a dose-dependent manner in the MiAEC and HiAEC treated groups compared with the Vehicle group (Fig. 9A). However, protein expression levels in the NF-κB signaling pathway were significantly inhibited under the same conditions, where the protein expression levels of p-NF-κB and p-IκB-α were significantly lower in the AEC treated group compared with the Vehicle group (Fig. 9B). Therefore, the inhibitory effects of AEC on CT26 tumor growth could be linked to the upregulation of tumor suppression-related proteins through the inhibition of the NF-κB signaling pathway in CT26 tumors in BALB/cKorl syngeneic mice.

A

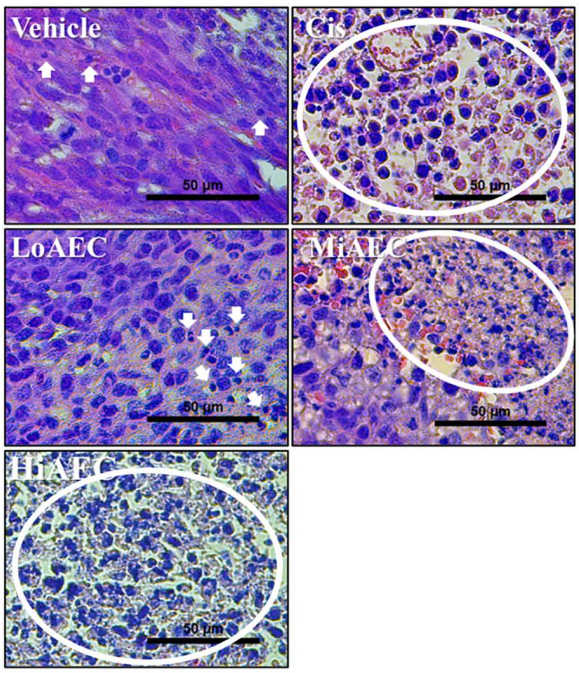

B

	Necrotic area	Spindle tumor cell	Vacuolated tumor cell	Foamy and plump tumor cell
Vehicle	+	+	+	+
Cis	+++	+	+	+
LoAEC	+	+	+	+
MiAEC	+	+	+	+
HiAEC	+++	+	+	+

Figure 5. Histological structure of CT26 tumors in BALB/cKorl syngeneic mice. (A) Histopathological structure of the tumor. Tumorigenic alterations, such as necrosis (white arrow and white circle), were demonstrated in H&E stained tumor sections at 400x magnification. (B) Assessment of the histopathological structure in the H&E stained tumor sections. The preparation of the H&E stained tissue sections was performed on five to six tumors per group; the pathological factors were analyzed twice for each stained tissue. AEC, aqueous extract of *Ecklonia cava*; Cis, cisplatin; Lo, low concentration; Mi, middle concentration; Hi, high concentration; H&E, hematoxylin and eosin.

Evaluation of the potential for the role of PT as the primary bioactive substance in AEC in CT26 cells. Finally, the anti-tumor effects of PT as the bioactive compound candidates in AEC were confirmed in CT26 cells. Changes in the cytotoxicity and apoptosis activation were assessed in CT26 cells after PT treatment. The viability of CT26 cells was significantly decreased in the PT treated groups compared with the No or Vehicle group (Fig. 10A). The number of cells stained with Ki67 protein were significantly decreased in the PT treated groups compared with the No or Vehicle groups (Fig. 10B). The PT treated groups in CT26 cells demonstrated an increase in the phosphorylation levels of ERK, JNK and p38 proteins compared with Vehicle group although the increased rate of JNK was the lowest among them (Fig. 10C). Also, similar enhancements in the protein expression levels of Bax/Bcl-2 and Cleaved Cas-3/Cas-3 were observed in the CT26 cells treated with PT and HiAEC compared with the No or Vehicle group (Fig. 10D). Therefore, PT in AEC can be considered one of the main bioactive compounds which exert an anti-tumor effect of AEC.

Discussion

Tannins are found in numerous parts of the plant, including the bark of trees, wood, leaves, fruits, seeds and roots, to protect them from fungi and bacteria (37). Based on these characteristics, numerous studies on the therapeutic effects of tannins have been reported. Among these, the anti-carcinogenic and anti-mutagenic potential of tannins have attracted considerable attention because their high antioxidative properties protect against cellular oxidative damage (38). The present study evaluated the anti-tumor effects and the molecular mechanisms of AEC in CT26 cells and CT26 tumors in BALB/cKorl syngeneic mice to identify a novel function of *E. cava*, which contains certain tannins, for tumor therapy. The results from the present study suggested that AEC had anti-tumor effects, including strong cytotoxicity, activation of apoptosis, suppression of cell proliferation, inhibition of migration ability and enhanced tumor suppression ability in CT26 colon cancer cells. Furthermore, the results from the PT treated CT26 cells indicated that PT was one of the bioactive component candidates with anti-tumor activity in AEC.

The AEC used in the present study was extracted from the same raw materials of *E. cava* as the tannin-enriched extract of *E. cava* used in a previous study (17). However, there was a difference in the extraction method, and this difference is hypothesized to be the cause of the difference in the phytochemicals content, radical scavenging activity and active compound content. In the present study, eleven bioactive compounds including triacontanoic acid, fucosterol, 9,12-octadecadienoic acid, aspartic acid, phloroglucinol, eckol, phlorofucofuroeckol, 6,6'-bieckol, fucodiphloroethanol G, docosanoic acid and dieckol were identified in AEC using LC-MS analyses. Identification of most of the aforementioned compounds were consistent with previous studies which identified novel bioactive compounds from *E. cava* (39,40,41). A total of forty-one compounds containing PT and other bioactive compounds were reported to have been detected in the total ion chromatograms of the sub-fractions of *E. cava* eluted with 30% MeOH and 70% MeOH (39). Previously, seven PTs and three sterol derivatives were purified from *E. cava* using the comprehensive spectral analysis for nuclear magnetic resonance and mass spectrometry data (40). Furthermore, the high pressure liquid chromatography peaks of eckol and dieckol were detected in the ethyl acetate fraction of *E. cava* (41). However, active compounds identified from *E. cava* differ between studies. In the present study, few compounds including triacontanoic acid, fucosterol, 9,12-octadecadienoic acid, docosanoic acid with low solubility were detected in AEC, which was extracted with water solvent (Fig. 1). Among these compounds, 9,12-octadecadienoic acid and docosanoic acid were also found in water extracts of *Cladosporium perangustum* and *Desmodium gangeticum* (42,43). These data demonstrated that the low water-soluble compounds could be extracted during an extraction process including a 100˚C boiling step. However, the present study had certain limitations in that it did not fully reflect the variation between batches in the separation and isolation of bioactive components because many bioactive components in marine plants are affected by numerous environmental conditions. Therefore, more studies

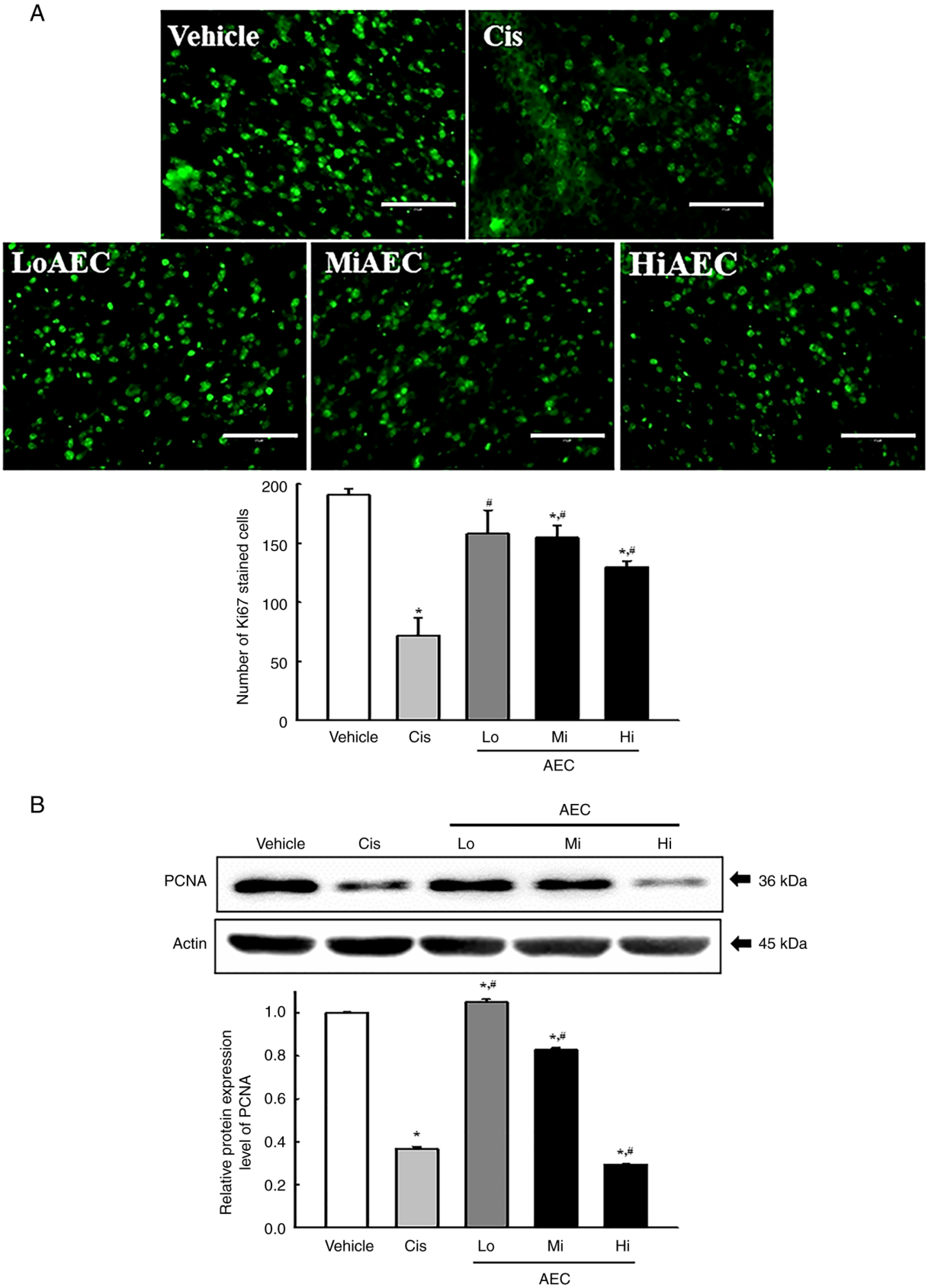

Figure 6. Protein expression levels of Ki67 and PCNA in CT26 tumors in BALB/cKorl syngeneic mice. (A) IF assays for Ki67. After IF staining, Ki67 positive cells were assessed in the total area of the field of view (67,500 mm^2) for each CT26 tumor section. The Ki67-stained slides were prepared for two to three tumors per group based on H&E staining results, and Ki67 positive cells was counted two view fields for each sample. Scale bar=75 μm. (B) PCNA protein analysis. After collecting the CT26 tumors, the band density for the specific protein was analyzed using densitometry. The tissue homogenates were prepared from two to three tumors per group based on the results of the weight measurement and H&E staining analysis, and the western blot was analyzed twice for each sample. The level of each protein was normalized to β-actin. The data was presented as the mean ± SD. *P<0.05 vs. Vehicle group. #P<0.05 vs. Cis group. PCNA, proliferating cell nuclear antigen; IF, immunofluorescence; AEC, aqueous extract of *Ecklonia cava*; Cis, cisplatin; Lo, low concentration; Mi, middle concentration; Hi, high concentration; H&E, hematoxylin and eosin.

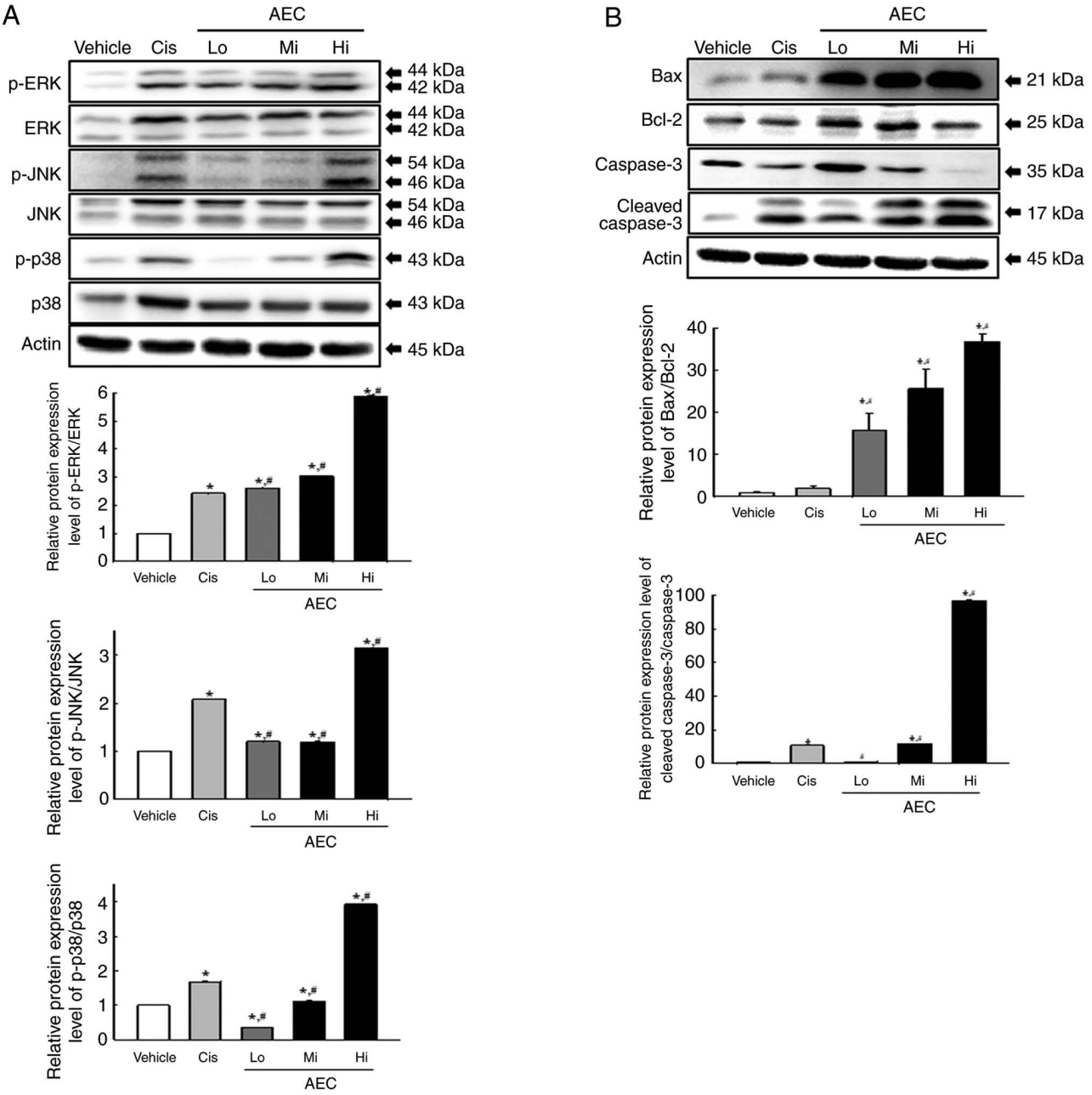

Figure 7. MAPK and Bax/Bcl-2 protein expression levels in a CT26 tumor in BALB/cKorl syngeneic mice. (A) MAPK signaling pathway analysis. After collecting the CT26 tumor, the protein expression levels of the phosphorylated form and unphosphorylated forms of the key members proteins were analyzed using specific antibodies and densitometry. (B) Bax/Bcl-2 pathway analysis. After collecting the CT26 tumors, the protein expression levels of Bax, Bcl-2, Cas-3 and Cleaved Cas-3 were assessed using specific antibodies and densitometry. The tissue homogenates were prepared from two to three tumors per group and western blot was analyzed twice for each sample. The level of each protein was normalized to β-actin. The data was presented as the mean ± SD. *P<0.05 vs. Vehicle group. $^{\#}$P<0.05 vs. Cis group. MAPK, mitogen-activated protein kinases; p, phosphorylated; AEC, aqueous extract of *Ecklonia cava*; Cis, cisplatin; Lo, low concentration; Mi, middle concentration; Hi, high concentration.

will be required to separate and isolate bioactive components of AEC and investigate their biological effects one by one.

Apoptosis is one of the targets for a potential anti-tumor drug because it is the best-studied model of programmed cell death of damaged, worthless or outdated cells (44). During these processes, the MEK/ERK and Bcl-2/Bax signaling pathways are deregulated in many human tumors, including pediatric leukemia (45). Certain compounds derived from *E. cava* exert different effects on the activation of apoptosis. Phloroglucinol did not induce cytotoxicity of endothelial progenitor cells at concentrations <100 μM (46). PT and PT enriched extracts induced significant cytotoxicity of ovarian cancer A2780 and SKOV3 cells (47). The number of apoptotic cells was increased after treatment with PT enriched extracts, while the expression levels of the pro-Cas-3, 8 and 9 proteins, and Bcl-2 and Bcl-xL decreased under the same conditions (47). Furthermore, similar effects on the stimulation of apoptosis for SKOV3 cells were reported using dieckol isolated from *E. cava* (16). The phloroglucinol derivative from *E. cava* induced apoptosis and increased the Cas-3/9 activity in breast cancer MCF-7 cells (7). The present study analyzed the changes in certain major factors related to cytotoxicity, the expression levels of

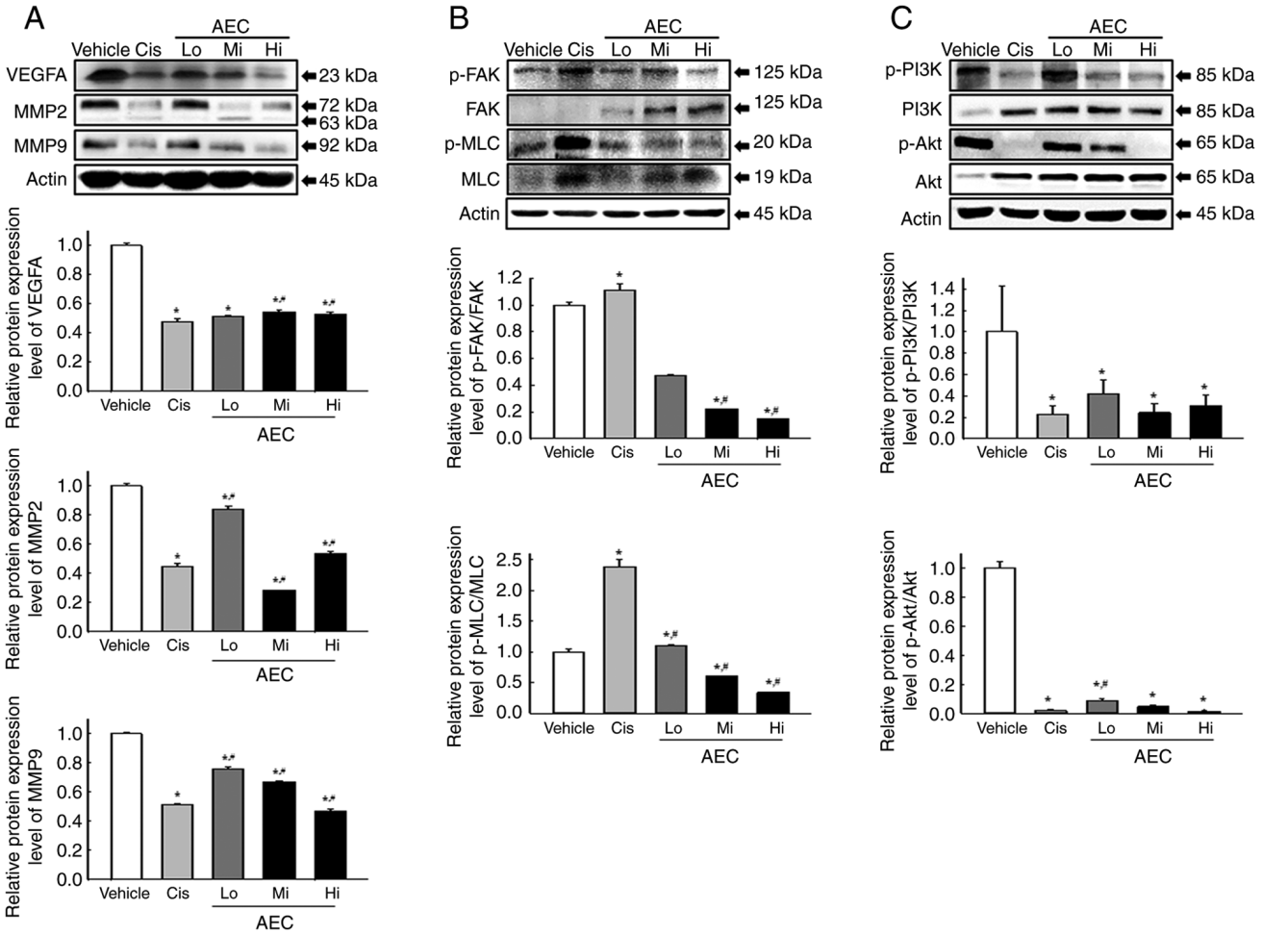

Figure 8. Analyses of the migration ability-related proteins in CT26 tumors of BALB/cKorl syngeneic mice. After collecting the CT26 tumor, the protein expression levels of (A) VEGFA, MMP2 and MMP9, (B) p-FAK, FAK, p-MLC and MLC, and (C) p-PI3K, PI3K, p-Akt and Akt in CT26 tumor homogenates were analyzed using specific antibodies and densitometry. The level of each protein was normalized to β-actin. The tissue homogenates was prepared from two to three tumors per group and western blots were analyzed twice for each sample. The data was presented as the mean ± SD. *P<0.05 vs. Vehicle group. #P<0.05 vs. Cis group. p, phosphorylated; AEC, aqueous extract of *Ecklonia cava*; Cis, cisplatin; Lo, low concentration; Mi, middle concentration; Hi, high concentration; MLC, myosin light chain; FAK, focal adhesion kinase; PI3K, phosphoinositide 3-kinases.

Bax/Bcl-2 and Cas-3, and the MAPK signaling pathway in CT26 cells and CT26 tumors in BALB/cKorl syngeneic mice after AEC treatment. The AEC treatment induced an increase in the number of apoptotic cells, and Bax/Bcl-2 and Cleaved Cas-3/Cas-3 protein expression levels in the cell line and solid tumor. These results were similar to those previously reported for PT, PT enriched extracts and dieckol treated ovarian cancer cells, even though the types of tumor cells were different in each study. The results from the present study indicated that AEC could effectively stimulate the apoptosis of colon cancer cells.

The proliferative activity of the cell population is typically determined using standard markers, including Ki67, PCNA and minichromosome maintenance proteins because their expression manifests during the proliferation of normal and neoplastic cells (48). In particular, the expression levels of the aforementioned markers was also reported in numerous malignant tumors, including multiple myeloma (49), prostate cancer (50) and breast cancer (51). They were significantly lower in tumors after treatment using various natural products, including grape seed proanthocyanidins extract, gallatannin and French maritime pine bark (52-54); however, the efficacy of *E. cava* extracts has not been previously reported to the best of our knowledge. High anti-proliferative activity was reported in MCF-7 breast cancer cells after treatment with the phloroglucinol derivative from *E. cava* (7). The present study evaluated the efficacy of *E. cava* extracts on the suppression of proliferative activity in CT26 tumors in BALB/cKorl syngeneic mice. The protein expression levels of Ki67 and PCNA decreased markedly in the AEC treated group. These results were consistent with the aforementioned, previous reports. Therefore, the results provided novel evidence that AEC could inhibit the proliferative activity of CT26 tumors in BALB/cKorl syngeneic mice by regulation of the Ki67 and PCNA proteins.

The present study evaluated the protein expression level of cell migration proteins and the MLC/FAK/Akt signaling pathway to investigate the inhibition effects of AEC on the migration ability of CT26 tumors. The AEC treated group exhibited markedly lower VEGFA, MMP2 and MMP9 protein expression levels and inhibition of the MLC/FAK/Akt signaling pathway in CT26 tumors in BALB/cKorl syngeneic mice compared with the control. These results on metastasis were similar to those of certain previous reports (55-61). The

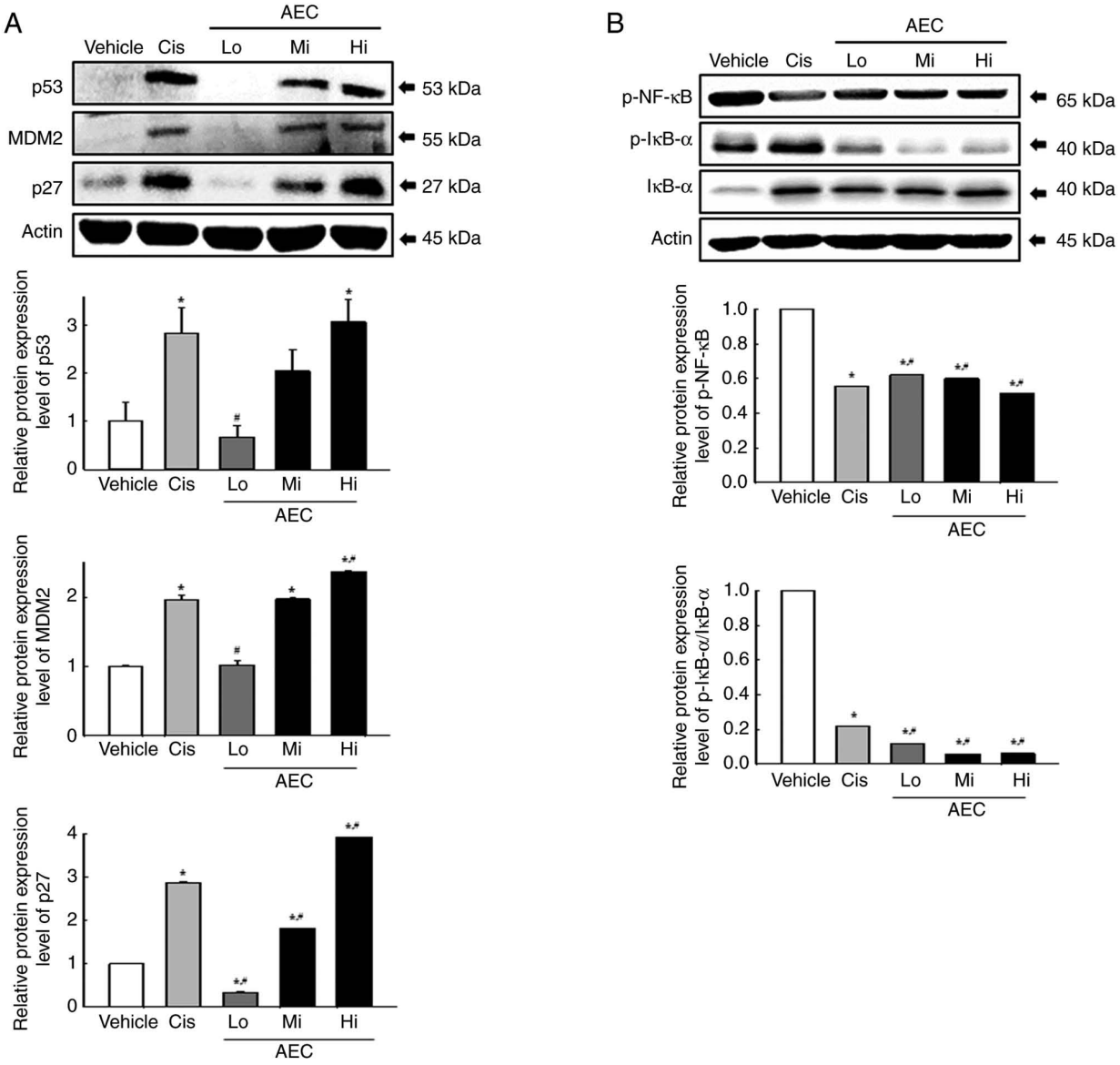

Figure 9. Analyses of tumor suppression-related proteins and NF-κB signaling pathway proteins in CT26 tumors in BALB/cKorl syngeneic mice. Protein expression levels of (A) p53, MDM2 and p27, and (B) p-NF-κB, p-IκB-α and IκB-α proteins in CT26 tumor homogenates were analyzed using specific antibodies. The level of each protein was normalized to β-actin. The tissue homogenates was prepared from two to three tumors per group and western blots were analyzed twice for each sample. The data was presented as the mean ± SD. *P<0.05 vs. Vehicle group. #P<0.05 vs. Cis group. p, phosphorylated; AEC, aqueous extract of *Ecklonia cava*; Cis, cisplatin; Lo, low concentration; Mi, middle concentration; Hi, high concentration; MDM2, mouse double minute 2.

metastatic process in the tumor tissue includes numerous molecular events, including the loss of cell-cell adhesion ability, alterations in the cell-matrix interaction, initiation of angiogenesis and degradation of the basement membrane and extracellular matrix (55,56). During the migration and invasion process, the PI3K/Akt mediated signaling pathway and the level of certain related proteins, such as MMPs and VEGF, can contribute as key regulators (57,58). A similar effect on the inhibition of metastasis was reported in previous studies that analyzed cancer cells treated with dieckol isolated from *E. cava*. Dieckol treatment induced a decrease in MMP2, MMP9, NF-κB and FAK expression and inhibited cell migration in human fibrosarcoma HT1080 cells (59,60). Similar effects, including the inhibition of gap closure and decreased MMP9 and VEGF expression, were reported in MCF-7 cells. In contrast, lung cancer cells treated with dieckol exhibited the suppression of migration, decreased N-cadherin levels and activation of key members in the PI3K/Akt signaling pathway (57,61). However, further research involving scratch and Transwell cell migration assays will be required to verify the inhibition effects of AEC on the migration ability of tumor cells based on the decrease in the expression of proteins involved in migration.

p53, a key tumor suppressor, and NF-κB, a key regulator of inflammation, are the major regulators of the physiological stress response (62). During this process, p53 and NF-κB proteins translocate from the cytoplasmic region to the nucleus and control the transcription of certain response genes (63,64). However, severe dysregulation on p53 and the NF-κB mediated pathway is commonly reported in cancer development and progression (64,65). In tumors, the constitutive activation of NF-κB causes chronic inflammation, which suppresses

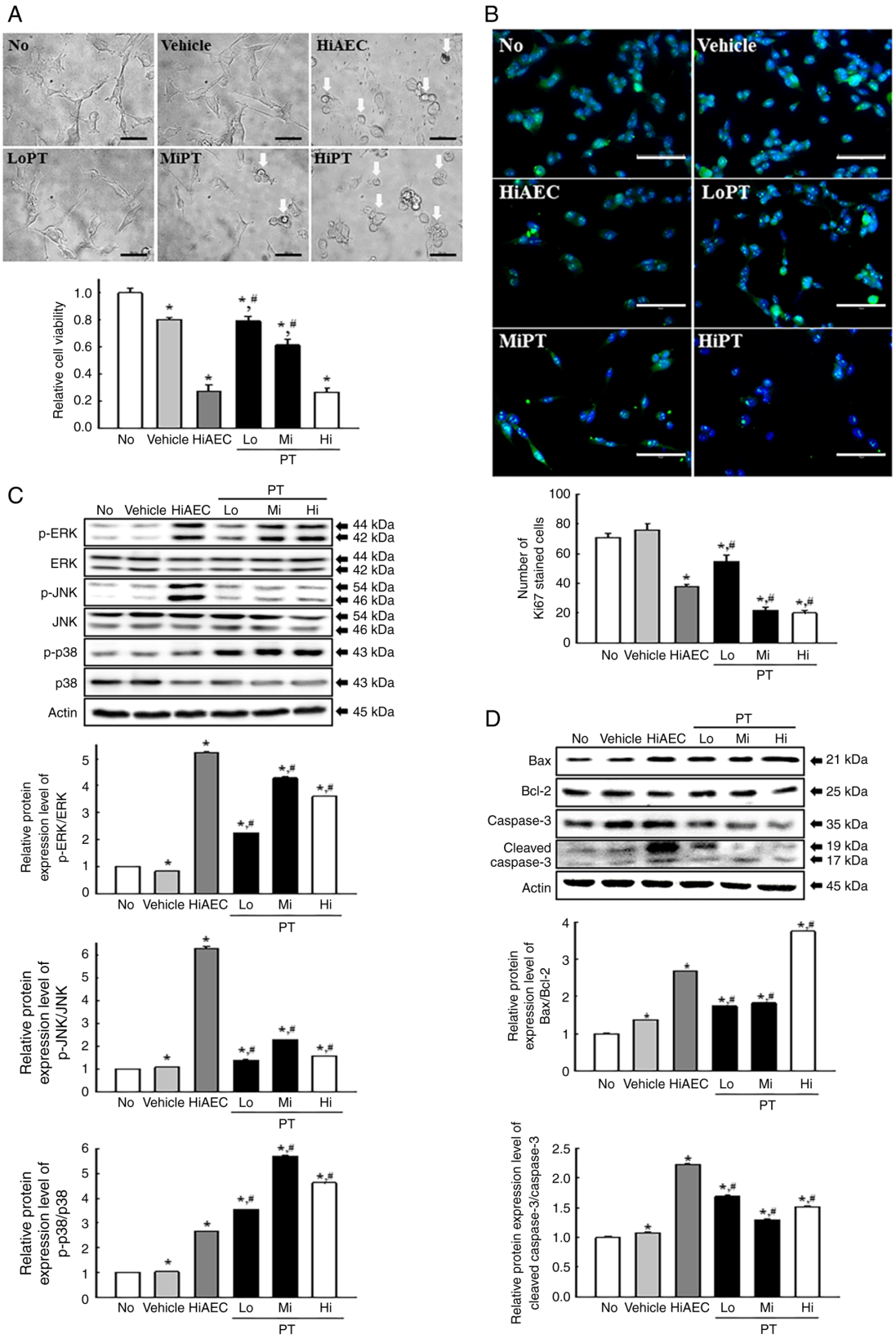

Figure 10. Anti-tumor effects of PT-treated CT26 cells. (A) Relative cell viability of PT in CT26 cells. After incubating CT26 cells with PT for 24 h, the morphology of the CT26 cells was observed under an inverted microscope at 400x magnification (Top). Scale bar=50 μm. An MTT assay based on the optical density of the solubilized formazan was performed on two to three wells per group, and the OD was measured twice for each sample (Bottom). (B) IF assays for Ki67. After IF staining, the number of Ki67 positive cells were counted in two field of views with total area of 67,500 mm^2 per field of view in each well. The Ki67-stained samples were prepared on two to three wells per group and Ki67 positive cells was counted twice for each sample. Scale bar=75 μm. (C) MAPK and (D) Bax/Bcl-2 signaling pathway analysis. After treatment with PT for 24 h, the expression of Bax, Bcl-2, Cas-3 and Cleaved Cas-3 proteins as well as p-ERK, ERK, p-JNK, JNK, p-p38 and p38 proteins were detected using specific antibodies. The cell homogenates were prepared on two to three dishes per group and western blots were analyzed twice for each sample. The data was presented as the mean ± SD. *P<0.05 vs. No group. $^\#$P<0.05 vs. Vehicle group. AEC, aqueous extract of *Ecklonia cava*; PT, phlorotannin; IF, immunofluorescence; MAPK, mitogen-activated protein kinases; p, phosphorylated; No, untreated; HiAEC, high concentration of AEC; Lo, low concentration; Mi, middle concentration; Hi, high concentration; p, phosphorylated.

the tumor suppressor activity of p53, even though they are in reciprocal negative regulation (66). To the best of our knowledge there have been few previous reports of the correlation between these two regulators and the anti-cancer effects of *E. cava*. Down-regulation of the NF-κB family and dependent activated genes were only reported in MCF-7 cells after exposure to one of the phloroglucinol derivatives from *E. cava* (7). The present study evaluated p53 protein expression levels and the NF-κB signaling pathway in CT26 tumors of AEC treated BALB/cKorl syngeneic mice to determine the effects of AEC on the physiological stress response. AEC treatment induced a marked increase in p53 protein expression levels and inhibited the NF-κB signaling pathway in CT26 tumors in BALB/cKorl syngeneic mice. The results of the present study provided the first evidence, to the best of our knowledge, that AEC may be associated with the regulation of the major regulators of the physiological stress response.

PTs are polymers composed of phloroglucinol (1,3,5-trihydroxybenzene) monomer units linked by different binding patterns. They have been reported in many marine brown algae including *E. cava*, *Ecklonia stolonifera* and *Ecklonia kurome* (67,36). PTs can be categorized into four subgroups based on the types of linkage; PTs with an ether linkage group (fuhalols and phlorethols), PTs with a phenyl linkage group (fucols), PTs with an ether and phenyl linkage group (fucophloroethols) and PTs with a dibenzodioxin linkage group (eckols) (36). Twelve compounds were previously reported as a subclass of PT from marine brown algae (5,68-70). PTs in particular is very abundant in *E. cava* compared with other brown algae (2). Therefore, PTs are considered to be one of major causes of the beneficial functions of *E. cava* although their content is low (36). The amount of PT (0.26% w/w) from *E. cava* detected in this study differed from that detected in previous studies. In the 95% EtOH extract of *E. cava* ~5.66% w/w of PT was detected and a slightly higher concentration (7.52% w/w) of PT was detected in the 70% EtOH extract of *Colonia cava* (Laminariales) and *Sargassum horneri* (Fucales) (71,72). It was hypothesized that that this difference was due to the difference in extraction solvents and extraction processes between studies.

Furthermore, the present study analyzed the role of PT as one of the bioactive compound candidates for the anti-tumor effects of AEC. The level of cytotoxicity increased by 11 percentage points to 52% at 600, 800 and 1,000 μg/ml of AEC, while those levels increased by 21 percentage points to 64% at 100, 150 and 200 μg/ml of PT. The anti-tumor effects of dieckol, one of the components of PT, was previously reported in numerous cancer cell lines. In human fibrosarcoma HT1080 cells, dieckol treatment (50 and 100 μg/ml) inhibited cell migration and invasion, intracellular ROS production, MMP2 and 9 expression, and the NF-kB signaling pathway (59,60). In human breast cancer MCF-7 cells, similar effects, including cell movement, MMP expression and apoptosis, were reported after the dieckol treatment (100, 200 and 400 μg/ml) (13,73). Furthermore, dieckol induced the inhibition of invasive and migratory properties and stimulated apoptosis, while it increased the activity of caspases 3, 8 and 9 (61). When comparing the anti-tumor effects of dieckol with those of AEC and PT, similar effects of dieckol on cytotoxicity were measured at relatively lower concentrations (50-400 μg/ml) than AEC and PT. Therefore, these results and previous studies indicated a possible correlation between AEC, PT and dieckol during the anti-tumor activity despite the limitations in comparing different studies directly.

The present study had certain limitations on the concentration analyses of active compounds in AEC. The six compounds that belong to PT were not quantified even though the total amount of PT was determined. In previous studies, however, the concentration of each compound was well quantified in water extract of *E. cava*. Among these compounds, the highest concentration (1.01 μg/mg) was detected in eckol, followed in order by dieckol (4.64 μg/mg), 6,6'-bieckol (4.64 μg/mg), 8,8'-bieckol (1.18 μg/mg), and phloroglucinol (0.18 μg/mg) (74). The differences in the concentration of bioactive compounds between individual plants should be fully considered to support the consistency of the concentration of various components between studies; however, the aforementioned values are provided to give an indication of non-quantified active compounds in the present study.

The results of the present study provided additional scientific evidence that AEC has anti-tumor effects associated with the cytotoxicity, activation of apoptosis, suppression of migration ability and enhancement of tumor suppression ability in CT26 cells or CT26 tumors in BALB/cKorl syngeneic mice. Moreover, AEC is a potential anti-tumor drug without significant toxicity and PT may be one of bioactive component candidates. However, despite the evidence provided based on scientific analysis strategies, the low anti-tumor activity of AEC is a weak point in developing a drug for humans. Nevertheless, further studies will be required to evaluate the effects of the single bioactive compounds and the molecular mechanisms responsible for the anti-tumor effects as well as to evaluate the possibility of using a combined treatment of standard chemotherapy and extracts.

Acknowledgements

The authors wish to thank Miss Jin Hyang Hwang, the animal technician, for directing animal care at the Laboratory Animal Resources Center in Pusan National University (Miryang, Republic of Korea).

Funding

This project was supported by a 2021 and 2022 grant of BIOREIN (Laboratory Animal Bio Resources Initiative) received from the Ministry of Food and Drug Safety (Republic of Korea). The present study was also supported by the BK21 FOUR Program through the National Research Foundation of Korea funded by the Ministry of Education, Korea (grant nos. F21YY8109033 and F22YY8109033).

Availability of data and materials

The datasets used and/or analyzed during the current study are available from the corresponding author on reasonable request.

Authors' contributions

JEG performed data curation and validation as well as design of the method. JEG, JEK and SHP performed the

formal analysis. The investigation was performed by JEG, JEK, SJL and YJC. YWC and HSL provided resources and determined the bioactive compounds of AEC. SIC and JTH reviewed and edited the manuscript, analyzed the data and discussed the results. DYH was a major contributor to the experimental design, funding management and wrote the original manuscript. All authors have read and agreed to the published version of the manuscript. JEG, JEK, SJL and YJC confirm the authenticity of all the raw data.

Ethics approval and consent to participate

The protocol for experimental animal study was reviewed and approved by the Pusan National University Institutional Animal Care and Use Committee (approval no. PNU-2020-0108).

Patient consent for publication

Not applicable.

Competing interests

The authors declare that they have no competing interests.

References

1. Maegawa M, Yokohoma Y and Aruga Y: Critical light conditions for young *Ecklonia cava* and *Eisenia bicyclis* with reference to photosynthesis. Hydrobiologia 151: 447-455, 1987.
2. Heo SJ, Park EJ, Lee KW and Jeon YJ: Antioxidant activities of enzymatic extracts from brown seaweeds. Bioresour Technol 96: 1613-1623, 2005.
3. Kang KA, Lee KH, Chae S, Zhang R, Jung MS, Lee Y, Kim SY, Kim HS, Joo HG, Park JW, *et al*: Eckol isolated from *Ecklonia cava* attenuates oxidative stress induced cell damage in lung fibroblast cells. FEBS Lett 579: 6295-6304, 2005.
4. Ahn GN, Kim KN, Cha SH, Song CB, Lee J, Heo MS, Yeo IK, Lee NH, Jee YH, Kim JS, *et al*: Antioxidant activities of phlorotannins purified from *Ecklonia cava* on free radical scavenging using ESR and H_2O_2-mediated DNA damage. Eur Food Res Technol 226: 71-79, 2007.
5. Li Y, Qian ZJ, Ryu B, Lee SH, Kim MM and Kim SK: Chemical components and its antioxidant properties in vitro: An edible marine brown alga, *Ecklonia cava*. Bioorg Med Chem 17: 1963-1973, 2009.
6. Artan M, Li Y, Karadeniz F, Lee SH, Kim MM and Kim SK: Anti-HIV-1 activity of phloroglucinol derivative, 6,6'-bieckol, from *Ecklonia cava*. Bioorg Med Chem 16: 7921-7926, 2008.
7. Kong CS, Kim JA, Yoon NY and Kim SK: Induction of apoptosis by phloroglucinol derivative from *Ecklonia cava* in MCF-7 human breast cancer cells. Food Chem Toxicol 47: 1653-1658, 2009.
8. Athukorala Y and Jeon YJ: Screening for angiotensin 1-converting enzyme inhibitory activity of *Ecklonia cava*. Prev Nutr Food Sci 10: 134-139, 2005.
9. Jung WK, Ahn YW, Lee SH, Choi YH, Kim SK, Yea SS, Choi I, Park SG, Seo SK, Lee SW and Choi IW: *Ecklonia cava* ethanolic extracts inhibit lipopolysaccharide-induced cyclooxygenase-2 and inducible nitric oxide synthase expression in BV2 microglia via the MAP kinase and NF-kappaB pathways. Food Chem Toxicol 47: 410-417, 2009.
10. Lee SH, Li Y, Karadeniz F, Kim MM and Kim SK: α-Glycosidase and α-amylase inhibitory activities of phloroglucinal derivatives from edible marine brown alga, *Ecklonia cava*. J Sci Food Agric 89: 1552-1558, 2009.
11. Ahn JH, Yang YI, Lee KT and Choi JH: Dieckol, isolated from the edible brown algae *Ecklonia cava*, induces apoptosis of ovarian cancer cells and inhibits tumor xenograft growth. J Cancer Res Clin Oncol 141: 255-268, 2015.
12. Zhang C, Li Y, Shi X and Kim SK: Inhibition of the expression on MMP-2, 9 and morphological changes via human fibrosarcoma cell line by 6,6'-bieckol from marine alga *Ecklonia cava*. BMB Rep 43: 62-68, 2010.
13. Kim EK, Tang Y, Kim YS, Hwang JW, Choi EJ, Lee JH, Lee SH, Jeon YJ and Park PJ: First evidence that *Ecklonia cava*-derived dieckol attenuates MCF-7 human breast carcinoma cell migration. Mar Drugs 13: 1785-1797, 2015.
14. Sadeeshkumar V, Duraikannu A, Ravichandran S, Kodisundaram P, Fredrick WS and Gobalakrishnan R: Modulatory efficacy of dieckol on xenobiotic-metabolizing enzymes, cell proliferation, apoptosis, invasion and angiogenesis during NDEA-induced rat hepatocarcinogenesis. Mol Cell Biochem 433: 195-204, 2017.
15. Athukorala Y, Kim KN and Jeon YJ: Antiproliferative and antioxidant properties of an enzymatic hydrolysate from brown alga, *Ecklonia cava*. Food Chem Toxicol 44: 1065-1074, 2006.
16. Ahn G, Lee W, Kim KN, Lee JH, Heo SJ, Kang N, Lee SH, Ahn CB and Jeon YJ: A sulfated polysaccharide of *Ecklonia cava* inhibits the growth of colon cancer cells by inducing apoptosis. EXCLI J 14: 294-306, 2015.
17. Kim JE, Choi YJ, Lee SJ, Gong JE, Lee YJ, Sung JE, Jung YS, Lee HS, Hong JT and Hwang DY: Antioxidant activity and laxative effects of tannin-enriched extract of *Ecklonia cava* in loperamide-induced constipation of SD rats. PLoS One 16: e0246363, 2021.
18. Lee HS, Kim SW, Oak C, Kang HW, Oh J, Jung MJ, Kim SB, Won JH and Lee KD: Rabbit model of tracheal stenosis using cylindrical diffuser. Lasers Surg Med 49: 372-379, 2017.
19. Lee HS, Jeong MS, Ko SC, Heo SY, Kang HW, Kim SW, Hwang CW, Lee KD, Oak C, Jung MJ, *et al*: Fabrication and biological activity of polycaprolactone/phlorotannin endotracheal tube to prevent tracheal stenosis: An in vitro and in vivo study. J Biomed Mater Res B Appl Biomater 108: 1046-1056, 2020.
20. Gutfinger T: Polyphenols in olive oils. J Am Oil Chem Soc 58: 966-968, 1981.
21. Xu ML, Hu JH, Wang L, Kim HS, Jin CW and Cho DH: Antioxidant and anti-diabetes activity of extracts from *Machilus thunbergii S. et Z*. Korean J Medicinal Crop Sci 18: 34-39, 2010.
22. Price ML, Hagerman AE and Butler LG: Tannin content of cowpeas, chickpeas, pigeon peas, and mung beans. J Agric Food Chem 28: 459-461, 1980.
23. Go J, Kim JE, Koh EK, Song SH, Sung JE, Lee HA, Lee YH, Lim Y, Hong JT and Hwang DY: Protective effect of gallotannin-enriched extract isolated from *Galla rhois* against CCl4-induced hepatotoxicity in ICR mice. Nutrients 8: 107, 2016.
24. Catarino MD, Fernandes I, Oliveira H, Carrascal M, Ferreira R, Silva AMS, Cruz MT, Mateus N and Cardoso SM: Antitumor activity of *Fucus vesiculosus*-derived phlorotannins through activation of apoptotic signals in gastric and colorectal tumor cell lines. Int J Mol Sci 22: 7604, 2021.
25. Yu JW, Bhattacharya S, Yanamandra N, Kilian D, Shi H, Yadavilli S, Katlinskaya Y, Kaczynski H, Conner M, Benson W, *et al*: Tumor-immune profiling of murine syngeneic tumor models as a framework to guide mechanistic studies and predict therapy response in distinct tumor microenvironments. PLoS One 13: e0206223, 2018.
26. Hsieh YH, Wu CJ, Chow KP, Tsai CL and Chang YS: Electroporation-mediated and EBV LMP1-regulated gene therapy in a syngenic mouse tumor model. Cancer Gene Ther 10: 626-636, 2003.
27. Park HR, Jo SK, Cho HH and Jung U: Synergistic Anti-cancer Activity of MH-30 in a murine melanoma model treated with cisplatin and its alleviated effects against cisplatin-induced toxicity in mice. In Vivo 34: 1845-1856, 2020.
28. Noto FK, Sangodkar J, Adedeji BT, Moody S, McClain CB, Tong M, Ostertag E, Crawford J, Gao X, Hurst L, *et al*: The SRG rat, a Sprague-Dawley Rag2/Il2rg double-knockout validated for human tumor oncology studies. PLoS One 15: e0240169, 2020.
29. Na K, Li K, Sang T, Wu K, Wang Y and Wang X: Anticarcinogenic effects of water extract of sporoderm-broken spores of *Ganoderma lucidum* on colorectal cancer *in vitro* and *in vivo*. Int J Oncol 50: 1541-1554, 2017.
30. Erickson RL, Blevins CE, Souza Dyer C and Marx JO: Alfaxalone-Xylazine anesthesia in laboratory mice (*Mus musculus*). J Am Assoc Lab Anim Sci 58: 30-39, 2019.

31. Best I, Casimiro-Gonzales S, Portugal A, Olivera-Montenegro L, Aguilar L, Muñoz AM and Ramos-Escudero F: Phytochemical screening and DPPH radical scavenging activity of three morphotypes of *Mauritia flexuosa* L.f. from Peru, and thermal stability of a milk-based beverage enriched with carotenoids from these fruits. Heliyon 6: e05209, 2020.
32. Mazumder K, Nabila A, Aktar A and Farahnaky A: Bioactive variability and in vitro and in vivo antioxidant activity of unprocessed and processed flour of nine cultivars of Australian lupin species: A comprehensive substantiation. Antioxidants (Basel) 9: 282, 2020.
33. Liu DZ, Lin YS and Hou WC: Monohydroxamates of aspartic acid and glutamic acid exhibit antioxidant and angiotensin converting enzyme inhibitory activities. J Agric Food Chem 52: 2386-2390, 2004.
34. Manandhar B, Paudel P, Seong SH, Jung HA and Coi JS: Characterizing eckol as a therapeutic aid: A systematic review. Mar Drugs 17: 361, 2019.
35. Fernando IP, Kim M, Son KT, Jeong Y and Jeon YJ: Antioxidant activity of marine algal polyphenolic compounds: A mechanistic approach. J Med Food 19: 615-628, 2016.
36. Li Y, Wijesekara I, Li Y and Kim S: Phlorotannins as bioactive agents from brown algae. Process Biochem 46: 2219-2224, 2011.
37. Aristri MA, Lubis MAR, Iswanto AH, Fatriasari W, Sari RK, Antov P, Gajtanska M, Papadopoulos AN and Pizzi A: Bio-based polyurethane resins derived from tannin: Source, synthesis, characterization, and application. Forests 12: 1516-1538, 2021.
38. Chung KT, Wong TY, Wei CI, Huang YW and Lin Y: Tannins and human health: A review. Crit Rev Food Sci Nutr 38: 421-464, 1998.
39. Cho HM, Doan TP, Ha TKQ, Kim HW, Lee BW, Pham HTT, Cho TO and Oh WK: Dereplication by high-performance liquid chromatography (HPLC) with quadrupole-time-of-flight mass spectroscopy (qTOF-MS) and antiviral activities of phlorotannins from *Ecklonia cava*. Mar Drugs 17: 149, 2019.
40. Lee JH, Ko JY, Oh JY, Kim CY, Lee HJ, Kim J and Jeon YJ: Preparative isolation and purification of phlorotannins from *Ecklonia cava* using centrifugal partition chromatography by one-step. Food Chem 158: 433-437, 2014.
41. Lee JW, Seok JK and Boo YC: *Ecklonia cava* extract and dieckol attenuate cellular lipid peroxidation in keratinocytes exposed to PM10. Evid Based Complement Alternat Med 2018: 8248323, 2018.
42. Govindappa M, Lavanya M, Aishwarya P, Pai K, Lunked P, Hemashekhar B, Arpitha BM, Ramachandra YL and Raghavendra VB: Synthesis and characterization of endophytic fungi, *Cladosporium perangustum* mediated silver nano-particles and their antioxidant, anticancer and nano-toxicological study. Bionanoscience 10: 928-941, 2020.
43. Kurian GA and Paddikkala J: Oral delivery of insulin with *Desmodium gangeticum* root aqueous extract protects rat hearts against ischemia reperfusion injury in streptozotocin induced diabetic rats. Asian Pac J Trop Med 3: 94-100, 2010.
44. Baig S, Seevasant I, Mohamad J, Mukheem A, Huri HZ and Kamarul T: Potential of apoptotic pathway-targeted cancer therapeutic research: Where do we stand? Cell Death Dis 7: e2058, 2016.
45. Vitagliano O, Addeo R, D'Angelo V, Indolfi C, Indolfi P and Casale F: The Bcl-2/Bax and Ras/Raf/MEK/ERK signaling pathways: Implications in pediatric leukemia pathogenesis and new prospects for therapeutic approaches. Expert Rev Hematol 6: 587-597, 2013.
46. Kwon YH, Jung SY, Kim JW, Lee SH, Lee JH, Lee BY and Kwon SM: Phloroglucinol inhibits the bioactivities of endothelial progenitor cells and suppresses tumor angiogenesis in LLC-tumor-bearing mice. PLoS One 7: e33618, 2012.
47. Yang YI, Ahn JH, Choi YS and Choi JH: Brown algae phlorotannins enhance the tumoricidal effect of cisplatin and ameliorate cisplatin nephrotoxicity. Gynecol Oncol 136: 355-364, 2015.
48. Juríková M, Danihel Ľ, Polák Š and Varga I: Ki67, PCNA, and MCM proteins: Markers of proliferation in the diagnosis of breast cancer. Acta Histochem 118: 544-552, 2016.
49. Alexandrakis MG, Passam FH, Kyriakou DS, Dambaki K, Niniraki M and Stathopoulos E: Ki-67 proliferation index: Correlation with prognostic parameters and outcome in multiple myeloma. Am J Clin Oncol 27: 8-13, 2004.
50. Li R, Heydon K, Hammond ME, Grignon DJ, Roach M III, Wolkov HB, Sandler HM, Shipley WU and Pollack A: Ki-67 staining index predicts distant metastasis and survival in locally advanced prostate cancer treated with radiotherapy: An analysis of patients in radiation therapy oncology group protocol 86-10. Clin Cancer Res 10: 4118-4124, 2004.
51. Urruticoechea A, Smith IE and Dowsett M: Proliferation marker Ki-67 in early breast cancer. J Clin Oncol 23: 7212-7220, 2005.
52. Abd Eldaim MA, Tousson E, El Sayed IET, Abd El-Aleim AEH and Elsharkawy HN: Grape seeds proanthocyanidin extract ameliorates Ehrlich solid tumor induced renal tissue and DNA damage in mice. Biomed Pharmacother 115: 108908, 2019.
53. Al-Halabi R, Bou Chedid M, Abou Merhi R, El-Hajj H, Zahr H, Schneider-Stock R, Bazarbachi A and Gali-Muhtasib H: Gallotannin inhibits NFκB signaling and growth of human colon cancer xenografts. Cancer Biol Ther 12: 59-68, 2011.
54. Kimura Y and Sumiyoshi M: French maritime pine bark (*Pinus maritima* Lam.) extract (Flavangenol) prevents chronic UVB radiation-induced skin damage and carcinogenesis in melanin-possessing hairless mice. Photochem Photobiol 86: 955-963, 2010.
55. Folkman J and Shing Y: Angiogenesis. J Biol Chem 267: 10931-10934, 1992.
56. Martin TA and Jiang WG: Loss of tight junction barrier function and its role in cancer metastasis. Biochim Biophys Acta 1788: 872-891, 2009.
57. Kim D, Kim S, Koh H, Yoon SO, Chung AS, Cho KS and Chung J: Akt/PKB promotes cancer cell invasion via increased motility and metalloproteinase production. FASEB J 15: 1953-1962, 2001.
58. Yang SX, Polley E and Lipkowitz S: New insights on PI3K/AKT pathway alterations and clinical outcomes in breast cancer. Cancer Treat Rev 45: 87-96, 2016.
59. Zhang C, Li Y, Qian ZJ, Lee SH, Li YX and Kim SK: Dieckol from *Ecklonia cava* regulates invasion of human fibrosarcoma cells and modulates MMP-2 and MMP-9 expression via NF-κB pathway. Evid Based Complement Alternat Med 2011: 140462, 2011.
60. Park SJ and Jeon YJ: Dieckol from *Ecklonia cava* suppresses the migration and invasion of HT1080 cells by inhibiting the focal adhesion kinase pathway downstream of Rac1-ROS signaling. Mol Cells 33: 141-149, 2012.
61. Wang CH, Li XF, Jin LF, Zhao Y, Zhu GJ and Shen WZ: Dieckol inhibits non-small-cell lung cancer cell proliferation and migration by regulating the PI3K/AKT signaling pathway. J Biochem Mol Toxicol 33: e22346, 2019.
62. Gudkov AV, Gurova KV and Komarova EA: Inflammation and p53: A tale of two stresses. Genes Cancer 2: 503-516, 2011.
63. Lane D and Levine A: p53 Research: The past thirty years and the next thirty years. Cold Spring Harb Perspect Biol 2: a000893, 2010.
64. Karin M: Nuclear factor-kappaB in cancer development and progression. Nature 441: 431-436, 2006.
65. Levine AJ and Oren M: The first 30 years of p53: Growing ever more complex. Nat Rev Cancer 9: 749-758, 2009.
66. Kawauchi K, Araki K, Tobiume K and Tanaka N: Loss of p53 enhances catalytic activity of IKKbeta through O-linked beta-N-acetyl glucosamine modification. Proc Natl Acad Sci USA 106: 3431-3436, 2009.
67. Pal Singh I and Bharate SB: Phloroglucinol compounds of natural origin. Nat Prod Rep 23: 558-591, 2006.
68. Yoon NY, Chung HY, Kim H and Choi J: Acetyl- and butyryl-cholinesterase inhibitory activities of sterols and phlorotannins from *Ecklonia stolonifera*. Fish Sci 74: 200-207, 2008.
69. Nagayama K, Shibata T, Fujimoto K, Honjo T and Nakamura T: Algicidal effect of phlorotannins from the brown alga *Ecklonia kurome* on red tide microalgae. Aquaculture 218: 601-611, 2003.
70. Yoon NY: Cholinestarase and lens aldose reductase inhibitory activities of phlorotannins from *Ecklonia stolonifera* and their protective effects on tacrine induced hepatotoxicity and hyperlipidemic rat models. Ph.D. Thesis, Pukyong National University, Korea 4: 111, 2008.
71. Kim MM, Ta QV, Mendis E, Rajapakse N, Jung WK, Byun HG, Jeon YJ and Kim SK: Phlorotannins in *Ecklonia cava* extract inhibit matrix metalloproteinase activity. Life Sci 79: 1436-1443, 2006.
72. Sanjeewa KKA, Fernando IPS, Kim SY, Kim WS, Ahn G, Jee Y and Jeon YJ: *Ecklonia cava* (Laminariales) and *Sargassum horneri* (Fucales) synergistically inhibit the lipopolysaccharide-induced inflammation via blocking NF-κB and MAPK pathways. Algae 34: 45-56, 2019.
73. You SH, Kim JS and Kim YS: Apoptosis and cell cycle arrest in two human breast cancer cell lines by dieckol isolated from *Ecklonia cava*. J Breast Dis 6: 39-45, 2018.
74. Yang H, Lee SY, Lee SR, Pyun BJ, Kim HJ, Lee YH, Kwon SW, Suh DH, Lee CH, Hong EJ and Lee HW: Therapeutic effect of *Ecklonia cava* extract in letrozole-induced polycystic ovary syndrome rats. Front Pharmacol 9: 1325, 2018.